

3rd SFERA-III* / 16th SOLLAB Doctoral Colloquium 2022

September 12th – 14th 2022
ETH Zurich, Zurich, Switzerland



Book of Abstracts

* This project has received funding from the European Union's Horizon2020 Research and Innovation programme under grant agreement n°823802

Doctoral Colloquium

September 12th – 14th 2022

Monday, September 12th

08:30 – 09:00 **Registration** (collecting of name tag, signing in)
inside HG F3

09:00 – 09:10 **Opening and Welcome**
by Daniel Notter and Prof. Aldo Steinfeld, ETH Zurich (Organizers)

Session 1: Solar Systems

Chair: Prof. Manuel Romero, IMDEA

09:10 – 09:30 **Estimating predictive uncertainties of machine learning applications on solar tower power plants**

Leon Sievers, DLR

09:30 – 09:50 **Coupled Optimization of Design and Operation for Complex Hybrid Solar Power Systems**

Matthias Loevenich, DLR

09:50 – 10:10 **Techno-economic comparison of integrated CSP/PV concepts for pure electricity generation and combined heat and electricity generation**

Moritz Ruhwedel, DLR

10:10 – 10:30 **Analysis of solar power plant data for optimization of annual yield tools**

Tim Kotzab, DLR

10:30 – 11:00 **Coffee break**

11:00 – 11:20 **Potential applications of CSP technology in high-temperature industrial processes in Chile**

Juan Sebastián Zuleta Marin, Fraunhofer ISE

11:20 – 11:40 **Application of AI methods to improve Operation and maintenance of CSP power plants**

Thomas Kraft, Fraunhofer ISE

Session 2: Solar Optics

Chairs: Dr. Alain Dollet, PROMES-CNRS / Dr. Ricardo Sanchez, CIEMAT

11:40 – 12:00 **Evaluation of equipment for outdoor reflector measurements in CSP solar fields**

Johannes Wette, CIEMAT-PSA

12:00 – 12:20 **Characterizations and tests on the new Fresnel solar furnace testing platform at the Plataforma Solar de Almeria**
Noelia Estremera-Pedriza, CIEMAT-PSA

12:20 – 14:00 **Lunch** (*individually*)

14:00 – 14:20 **Approach for modelling the thermal performance of a Linear Fresnel Collector with a Trapezoidal Cavity Multi-tube Receiver**
Sergio Alcalde-Morales, CIEMAT-PSA

14:20 – 14:40 **Deep learning inversion of a raytracer**
Jan Lewen, DLR

14:40 – 15:00 **A purely data-driven deep learning digital twin approach for a heliostat field for flux density predictions**
Mathias Kuhl, DLR

15:00 – 15:20 **Geometric optimization of linear Fresnel collectors for solar thermal electricity**
André Santos, UEVORA

15:20 – 15:50 **Coffee break**

Session 3: Solar Receivers (Part A)

Chair: Prof. Robert Pitz-Paal, DLR

15:50 – 16:10 **Numerical Simulation of Pressure Drop in Wire Mesh Absorbers with Fixed Porosity**
Daniel Sanchez, CIEMAT-PSA

16:10 – 16:30 **Optimization of Spinel Absorber Coatings for CSP Particle Receivers**
Meryem Farchado, CIEMAT-PSA

16:30 – 16:50 **Numerical simulation of Improved Design for an Integrated Receiver and Storage system for CSP applications**
Christos Tengeris, CYI

16:50 – 17:00 **Closing remarks**

18:30 – 22:00 **Social Activity (Part 1)**
Dinner in Dozentenfoyer

Tuesday, September 13th**Session 4: Solar Fuels and Materials**

Chairs: Prof. Christian Sattler, DLR / Dr. Martin Roeb, DLR

09:00 – 09:20 Photocatalytic hydrogen production by natural solar radiation at pilot scale

Joyce Gloria Villachica Llamosas, CIEMAT-PSA

09:20 – 09:40 Sweeoped, Open, Moving Particle Reactor with Intrinsic Heat Recovery for Solar Thermochemical Hydrogen Production

Anika Weber, DLR

09:40 – 10:00 Reactor and system modelling for solar production of ethylene from H₂O and CO₂

David Brust, DLR

10:00 – 10:20 Get the right feature: Tailoring of material properties by Sr content in Ca_{1-x}Sr_xMnO_{3-δ}

Lena Klaas, DLR

10:20 – 11:00 Coffee break**11:00 – 11:20 Computational screening and experimental validation of binary and ternary metal nitrides for the solar-driven thermochemical production of green ammonia**

Daniel Notter, ETH

11:20 – 11:40 Dry Redox Reforming

Mario Zuber, ETH

11:40 – 12:00 Fully-automated Solar Fuel System for the Thermochemical Production of Syngas from H₂O and CO₂ applicable for Methanol or Fischer-Tropsch Synthesis

Remo Schächli, ETH

12:00 – 12:20 Solar calcination of non-metallic minerals: metakaoline production to synthesize zeolites

Pelin Paşabeyoğlu, METU

12:20 – 14:00 Lunch (individually)**14:00 – 14:20 Experimental Assessment of Solar Methane Pyrolysis in a Molten-Tin Bubble Column Reactor**

Malek Msheik, PROMES-CNRS

14:20 – 14:40 Modelling and Performance Analysis of a SOE System integrating PV, Concentrating Solar Heat and Thermal Energy Storage

Beatriz Herrero Badorrey, IMDEA

Session 5: Solar Water Treatment

Chair: Prof. Sixto Malato, CIEMAT-PSA

14:40 – 15:00 **Natural based solutions combined with solar advanced oxidation processes for wastewater recovery**

Alba Hernández-Zanoletty, CIEMAT-PSA

15:00 – 15:20 **Performance comparison of commercial membrane distillation modules operating in vacuum-assisted air gap configuration for brine concentration**

Isabel M^a Requena Requena, CIEMAT-PSA

15:20 – 15:50 *Coffee break*

15:50 – 16:10 **Modelling and automation of a multi-effect distillation plant for the optimal coupling with solar energy**

Juan Miguel Serrano Rodríguez, CIEMAT-PSA

16:10 – 16:30 **Implementation and evaluation of a solar photo-Fenton treatment plant for wastewater reclamation**

Elizabeth Gualda-Alonso, UAL

16:30 – 16:50 **New tertiary treatment for wastewater reclamation: Solar photo-Fenton combined with NaOCl**

Solaima Belachqer-El Attar, UAL

16:50 – 17:00 *Closing remarks*

Wednesday, September 14th**Session 6: Solar Receivers (Part B)**

Chair: Prof. Bernhard Hoffschmidt, DLR

09:00 – 09:20 High temperature pressure sealing: Utilization in a receiver-reactor cavity system

Estefanía Vega Puga, DLR

09:20 – 09:40 Numerical investigation of a helically coiled solar cavity receiver for simultaneous generation of superheated steam and air

Yasuki Kadohiro, DLR

09:40 – 10:00 Optimization of Porous Structures for Enhanced Radiation Heat Transfer Using a Voxel-Based Ray-Tracing Algorithm

Sebastian Sas Brunser, ETH

10:00 – 10:20 Development of an experimental testbed for Pressurised Gas Solar Receivers using a High Flux Solar Simulator

David D'Souza, IMDEA

10:20 – 10:30 *Closing remarks***10:30 – 11:00 *Coffee break*****11:00 – 12:30 Visit to Solar Mini-Refinery****12:30 – 14:00 *Lunch (individually)*****14:00 – 18:00 Social Activity (Part 2)**

Hike on Uetliberg

Book of Abstracts

Session 1: Solar Systems

Estimating predictive uncertainties of machine learning applications on solar tower power plants	1
Coupled Optimization of Design and Operation for Complex Hybrid Solar Power Systems	3
Techno-economic comparison of integrated CSP/PV concepts for pure electricity generation and combined heat and electricity generation.....	5
Analysis of solar power plant data for optimization of annual yield tools	7
Potential applications of CSP technology in high-temperature industrial processes in Chile	9
Application of AI methods to improve Operation and maintenance of CSP power plants	11

Session 2: Solar Optics

Evaluation of equipment for outdoor reflector measurements in CSP solar fields.....	13
Characterizations and tests on the new Fresnel solar furnace testing platform at the Plataforma Solar de Almeria	15
Approach for modelling the thermal performance of a Linear Fresnel Collector with a Trapezoidal Cavity Multi-tube Receiver	17
Deep learning inversion of a raytracer	19
A purely data-driven deep learning digital twin approach for a heliostat field for flux density predictions	21
Geometric optimization of linear Fresnel collectors for solar thermal electricity	22

Session 3: Solar Receivers (Part A)

Numerical Simulation of Pressure Drop in Wire Mesh Absorbers with Fixed Porosity.....	24
Optimization of Spinel Absorber Coatings for CSP Particle Receivers.....	26
Numerical simulation of Improved Design for an Integrated Receiver and Storage system for CSP applications.....	28

Session 4: Solar Fuels and Materials

Photocatalytic hydrogen production by natural solar radiation at pilot scale	29
Swepted, Open, Moving Particle Reactor with Intrinsic Heat Recovery for Solar Thermochemical Hydrogen Production.....	31
Reactor and system modelling for solar production of ethylene from H ₂ O and CO ₂	33
Get the right feature: Tailoring of material properties by Sr content in Ca _{1-x} Sr _x MnO _{3-δ}	35
Computational screening and experimental validation of binary and ternary metal nitrides for the solar-driven thermochemical production of green ammonia	36
Dry Redox Reforming.....	37
Fully-automated Solar Fuel System for the Thermochemical Production of Syngas from H ₂ O and CO ₂ applicable for Methanol or Fischer-Tropsch Synthesis.....	38



Solar calcination of non-metallic minerals: metakaoline production to synthesize zeolites 39

Experimental Assessment of Solar Methane Pyrolysis in a Molten-Tin Bubble Column Reactor 41

Modelling and Performance Analysis of a SOE System integrating PV, Concentrating Solar Heat and Thermal Energy Storage..... 43

Session 5: Solar Water Treatment

Natural based solutions combined with solar advanced oxidation processes for wastewater recovery 45

Performance comparison of commercial membrane distillation modules operating in vacuum-assisted air gap configuration for brine concentration. 47

Modelling and automation of a multi-effect distillation plant for the optimal coupling with solar energy 49

Implementation and evaluation of a solar photo-Fenton treatment plant for wastewater reclamation 51

New tertiary treatment for wastewater reclamation: Solar photo-Fenton combined with NaOCl 53

Session 6: Solar Receivers (Part B)

High temperature pressure sealing: Utilization in a receiver-reactor cavity system..... 55

Numerical investigation of a helically coiled solar cavity receiver for simultaneous generation of superheated steam and air 57

Optimization of Porous Structures for Enhanced Radiation Heat Transfer Using a Voxel-Based Ray-Tracing Algorithm..... 59

Development of an experimental testbed for Pressurised Gas Solar Receivers using a High Flux Solar Simulator..... 60

Estimating predictive uncertainties of machine learning applications on solar tower power plants

Leon Sievers, Bernhard Hoffschmidt, Daniel Maldonado Quinto

Institute of Solar Research, German Aerospace Center e.V. (DLR), l.sievers@dlr.de

When operating a solar tower power plant, a large number of parameters have to be tuned to optimize the throughput of thermal energy at the solar receiver. Each heliostat's orientation is controlled by two angles, representing the two movable axes. The entirety of all heliostats has to be controlled and orchestrated in such a way, that a desirable flux density distribution at the receiver is generated. In combination with the setting of the different components of air mass flow rate, these parameters control the behavior of the power plant. In general, the apparatus is thermally more efficient for higher temperatures of the heat medium, but a number of boundary conditions needs to be satisfied. The material properties of the receiver limit the operating temperature of the power plant as well as the spatial and temporal temperature gradients.

This work addresses the challenge of setting the large number of operating parameters in a way that allows for an efficient operation of a power plant while simultaneously guaranteeing safety of the plant. We want to approach this task using methods from artificial intelligence. A field of research, that deals with these safety-critical high-parametric optimization tasks, is called 'Safe AI'. In the last ten years, artificial intelligent methods have produced remarkable results in many fields like computer vision, natural language processing or complex board games. The application of machine learning techniques to optimization problems arising during the operation of solar tower power plants has been studied for some years now. Belhomme et al. have approached the optimization of heliostat aim point selection using an ant colony optimization algorithm [1]. They demonstrated the suitability of the algorithm to the aim point optimization problem and proposed its application in real-time due to its parallelizability. Pargmann et al. used pretrained deep neural networks and GANs to optimize the prediction of flux density distributions on the open volumetric receiver [2,3]. Their results indicate, that methods of artificial intelligence are very promising to excel at heliostat calibration. It becomes increasingly apparent, that artificial intelligence will play a vital role in the future of CSP.

However, machine learning methods often suffer from overconfidence and are not able to generalize to out-of-distribution samples, i.e. data that the algorithm has not seen in the learning process or is ill-defined for the task at hand. In many cases, artificial intelligence is capable of making sense of complex relations, but does not "know what it knows (and does

not know)”. It cannot estimate its own uncertainty and therefore is not able to indicate, when it is to be trusted and when it is not. To exploit the benefits of AI in safety-critical environments like aviation, autonomous driving and power plants, the safety of its predictions has to be guaranteed. Although this is a very hard problem in general, there are numerous approaches to quantify safety and security and to ensure them in artificial intelligence algorithms.

By using networks with radial basis functions, van Amersfoort et al. try to tackle the problem of epistemic uncertainty quantification in a scalable manner [4]. Lakshinarayanan et al. approach the same problem with Deep Ensemble models [5] and Charpentier et al. use an additional neural network (“PostNet”) to estimate uncertainty [6]. A further aspect of AI safety is calibration of neural networks. To ensure reliable AI, we need consistence of a model’s confidence outputs with reality. To this end, models can be calibrated following different procedures. Guo et al. offer temperature scaling, a single-parameter method with promising results [7]. Another branch of SafeAI is “Formal Verification”. Using rigorous mathematical proofs with techniques from function approximation, one tries to show certain properties of neural networks, e.g. stability of class predictions faced with adversarial attacks. Wang et al. deliver an insightful introduction to Interval Universal Approximation for Neural Networks in which they demonstrate the hardness of this mathematical problem [8].

The objective of my dissertation is to find artificial intelligence algorithms, that are beneficial to the optimization of operation trajectories in a solar tower power plant. In a further step, we want to apply an appropriate AI safety framework to verify consistent and secure behavior of said algorithms. In September, I hope to be able to present first results of this journey.

[1] B. Belhomme, R. Pitz-Paal, P. Schwarzbözl, *Journal of Solar Energy Engineering*, 136 (2014) 011005-1-011005-7.

[2] M. Pargmann, D. Maldonado Quinto, P. Schwarzbözl, R. Pitz-Paal, *Solar Energy*, 218 (2021) 48-56.

[3] M. Pargmann, D. Maldonado Quinto, S. Kesselheim, J. Ebert, R. Pitz-Paal, *Solar PACES 2021, Albuquerque, USA, 2021*.

[4] J. van Amersfoort, L. Smith, Y. W. The, Y. Gal, *CoRR*, 2003.02037 (2020).

[5] B. Lakshinarayanan, A. Pritzel, C. Blundell, *31st Conference on Neural Information Processing Systems (NIPS 2017)*, Long Beach, USA, 2017.

[6] B. Charpentier, D. Zügner, S. Günnemann, *34th Conference on Neural Information Processing Systems (NIPS 2020)*, Vancouver, Canada, 2020.

[7] C. Guo, G. Pleiss, Y. Sun, K. Q. Weinberger, *Proceedings of the 34th International Conference on Machine Learning*, Sydney, Australia, 2017.

[8] Z. Wang, A. Albargouthi, G. Prakriya, S. Jha, *Proceedings of the ACM on Programming Languages*, Vol. 1 (2018) No. CONF, Article 1

Coupled Optimization of Design and Operation for Complex Hybrid Solar Power Systems

Matthias Loevenich, Jürgen Dersch, Robert Pitz-Paal

*German Aerospace Center (DLR), Institute of Solar Research, Cologne, Germany.
matthias.loevenich@dlr.de*

The combination of photovoltaic (PV) and concentrated solar power (CSP) systems with thermal energy storage (TES) to hybrid solar power (HSP) systems makes solar electricity production dispatchable and cost competitive [1]. Furthermore, HSP systems can provide electricity and process heat simultaneously, which increases the attractiveness for applications such as decarbonization of the industry and solar fuel production. In order to exploit the full potential of HSP systems, optimal design and operation, depending on the site, demands and tariffs, are crucial [2]. Fluctuating solar energy resource induces a dispatch optimization to fulfill a load demand profile or to maximize profits according to a price schedule. An optimal design can only be evaluated depending on an optimal dispatch strategy and vice versa [3], resulting in a coupled optimization problem. The hybridization of solar power systems leads to an increasing number of degrees of freedom for design and operation as well as nonobvious interdependencies between components. Therefore, the optimization of design and operation becomes a nontrivial problem which is best solved using optimization algorithms [2].

The authors in [2, 4] introduce iterative methods to solve the coupled HSP optimization problem, using energy based and linearized model equations for the dispatch optimization and derivative-free stochastic algorithms for the design optimization. In contrast, state of the art models for techno-economic analysis of HSP systems are mass flow based, nonlinear and either equation based or data driven [5]. Model simplifications, as applied in [2] and [4], are often necessary to establish efficiently solvable optimization problems. Nevertheless, the results obtained with such simplified models are bound to the information loss caused by the simplification process. Additionally, the proposed optimization procedures can only be applied to HSP system configurations that can be represented by the simplified models created. Hence, we propose a more flexible optimization procedure to optimize the design and operation of HSP systems independently of the system configuration and model detail depth. The optimization framework shall be able to cope with mass flow based and nonlinear models, given in form of equations, data sets or combinations of both.

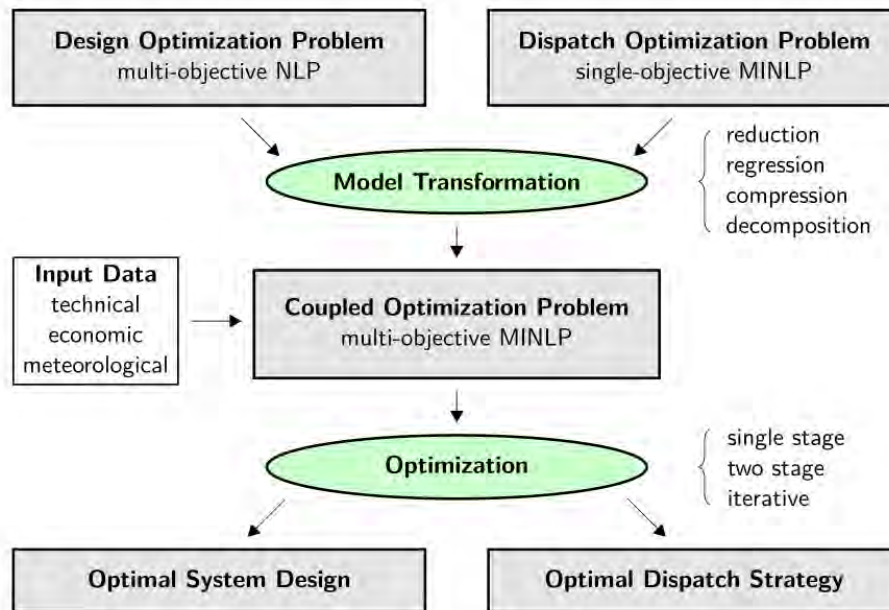


Fig. 1. Procedure for the coupled optimization of complex HSP systems

The proposed optimization procedure is summarized in Fig. 1. The coupled optimization problem is built automatically from the equation based or data driven models, chosen objectives and additional constraints, which define the design and dispatch optimization problems. The transformation process can consist of several steps such as regression and variable reduction to transform the given models and build the coupled optimization problem as a multi-objective mixed-integer nonlinear problem (MINLP). By choosing different methods depending on the type and detail depth of the given models, the transformation aims at building highly efficient new models with minimum information loss. The resulting optimization problem can be solved closely coupled with single or two stage deterministic solvers as well as slightly decoupled using an iterative approach. The iterative approach applies stochastic algorithms for the design optimization and the dispatch optimization is carried out for each design evaluation using deterministic or stochastic algorithms. The algorithms are chosen depending on the structure of the coupled optimization problem. This optimization procedure will enable the techno-economic analysis of HSP systems independent of the structure and model detail depth and will help to improve the performance of HSP and other renewable energy systems.

[1] J. Dersch, J. Inigo Labairu, L. Schomaker, M. Schlecht, L. Pfundmaier, F. Zimmermann, *Proc. of SolarPACES*, Online, 2021, 27.

[2] W. T. Hamilton, M. J. Wagner, A. M. Newman, R. J. Braun, *Proc. of SolarPACES, Daegu*, South Korea, 2019, 25.

[3] L. Bousselamti, et al., *J. Renewable Sustainable Energy*, 13 (2021) 013701.

[4] R. Bravo, D. Friedrich, *Solar Energy*, 164 (2018) 187-199.

[5] *SolarPACES Guideline for Bankable STE Yield Assessment 1st Edition*. T. Hirsch, et al., Spain, IEA Technology Collaboration Programme SolarPACES, 2017.

Techno-economic comparison of integrated CSP/PV concepts for pure electricity generation and combined heat and electricity generation

Moritz Ruhwedel^{1,a)}, Kai Gehrke², Florian Sutter¹, Eckhard Lüpfer¹, Robert Pitz-Paal¹

¹DLR – German Aerospace Center, Institute of Solar Research

²DLR – German Aerospace Center, Institute of Networked Energy Systems

^{a)}Moritz.Ruhwedel@dlr.de

Concentrating Solar Power (CSP) and Photovoltaics (PV) are both considered to be important sources of renewable energy. CSP/PV hybrid power plants optimize the electricity generation by shared use of both technologies on the same site but spatially separated. In this work the advantages of integrated CSP/PV concepts are compared, where instead of technical (and spatial) separation both components are integrated into the same solar field subsystems. The overall efficiency of CSP power plants can be increased by exploiting unutilized potentials of incoming solar radiation (e.g. spilled radiation, radiation that does not hit the aperture area, excess due to system reserves) with the added PV capabilities of the CSP components. Anticipated advantages due to the increased efficiency are reduction of levelized cost of energy (LCOE) and less required land area. Furthermore, material can be saved, if components can be used for both PV and CSP.

Such integrated CSP/PV components can additionally to pure electricity generation also be employed in the generation of process heat.

In this work three concepts for integrated CSP/PV components are compared to the reference case of separate CSP and PV installations. The concepts are shown in Fig.1 for a central receiver system. However, the application of the concepts is not limited to this case. The first concept is the integration of PV on the rear of the concentrating mirrors [1] (Concept 1: Bifacial rear PV in Fig.1). In Fig.1 it is realized by PV cells whose rear contacts are used as the mirrors for the CSP. Light scattered from the ground, the air or other mirrors is converted into electricity. Furthermore, during maintenance of the receiver, during clouds or when more solar energy is available than the receiver can take the rear-side PV can be turned upwards to face the sun to further increase the power output. The second concept uses spillage in the area around the receiver by PV [2] (Concept 2: Spillage-CPV in Fig.1). The third concept is the spectrally selective PVMirror as introduced by Yu et al. [3] (Concept 3: PVMirror in Fig.1), a specially coated PV module using only part of the incident light spectrum and the rest is reflected to the CSP receiver.

In the case of pure production of electricity, it is assumed for the reference concept that CSP and PV power plants coexist such that the energy produced by CSP makes up a specific fraction g of the energy produced by both of them. Therefore, total efficiency, total LCOE and total land usage can be calculated in dependence of g . The integrated CSP/PV concepts introduce additional amounts of energy produced by the PV components in the CSP power plants. This reduces the need for stand-alone PV power plants in order to maintain g . For use of all the concepts in the CSP power plants again total efficiency, total LCOE and total land usage can be calculated. These three parameters can then be compared in dependence of g . However, it has to be kept in mind that the PV of the integrated concepts will produce electricity at a different power profile than the stand-alone PV. Therefore, if a value of g optimizes the electricity production not only of the solar energy production, but of all forms of energy, using the reference concept, this value will differ from the value of g that optimizes the electricity production using the integrated concepts.

In the case of production of heat, it is assumed that only a specific restricted area, e.g. a roof of a factory, is available. The demand for heat should be assumed to be proportional to the available area. In the reference case CSP or non-concentrating solar thermal collectors should be used to generate the needed heat on a fraction of the area while the remaining space is utilized for electricity generation with PV. In this case the amount of additional producible electric energy can be calculated alongside with the LCOE of the produced heat and electricity. With the integrated CSP/PV concepts the needed amount of heat can be provided by CSP while additionally an amount of electric energy is generated by the PV of the integrated concepts on a fraction of the available area. The remaining area can be utilized using PV as in the reference case. Again, the amount of additional producible electric energy can be calculated alongside with the LCOE of the produced heat and electricity. These values then can be compared.

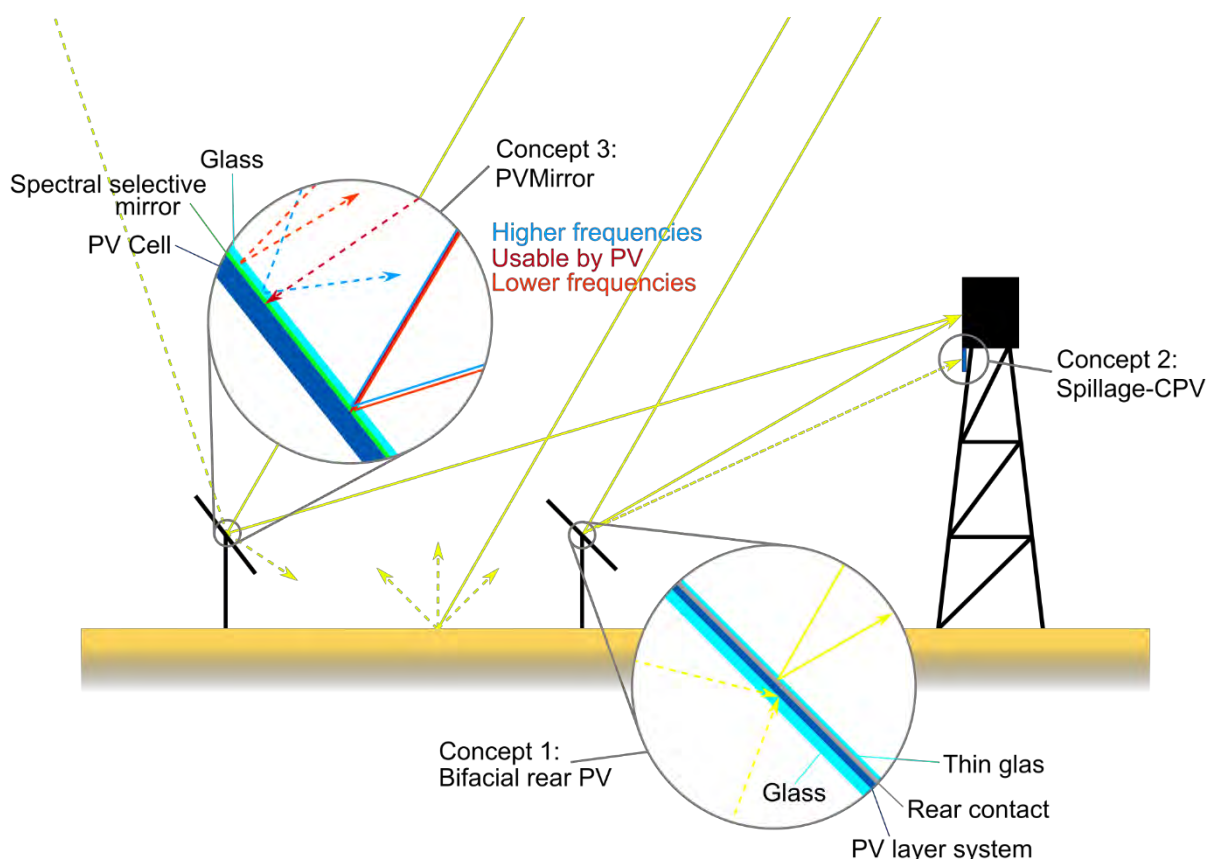


Fig.1: Schematic of the three integrated CSP/PV concepts (bifacial heliostat – spillage collector around receiver – selective mirror)

[1] M. Röger and F. Sutter. (2018). *Spiegelpanel für ein Solarkraftwerk sowie Solarkraftwerk*. DE Patent No. DE102018215657 (A1). Deutsches Patent- und Markenamt.

[2] K. C. Ho, C. O. McPheeters, P. R. Sharps, *AIP Conference Proceedings, Santiago de Chile*, Chile, 2018, 2033.

[3] Z. J. Yu, K. C. Fisher, B. M. Wheelwright, R. P. Angel, Z. C. Holman, *IEEE J. Photovoltaics*, 6 (2015) 1791–1799.

Analysis of solar power plant data for optimization of annual yield tools

Tim Kotzab, Tobias Hirsch, Robert Pitz-Paal

German Aerospace Center (DLR), Institute of Solar Research. tim.kotzab@dlr.de

Concentrating solar thermal power (STE) plants use collectors or heliostats to concentrate direct solar irradiation (DNI) to heat up a heat transfer fluid (HTF). The energy stored in the HTF can be used to generate electricity through a steam cycle process or for intermediate storage in thermal storage tanks. Thermal energy storage allows dispatchable power generation, which is attractive for large storage capacities in the range of 4 to 10 hours [1].

STE power plants are complex systems, which are made up of various components. The solar system, storage system, steam generator and electric generator are connected to form a complete power plant. STE power plants are designed and optimized for the specific location based on the requirements such as nominal electrical output and storage sizes, as well as local conditions such as DNI [2]. In order to amortize the initial investment costs over the lifetime of the plant, annual yield tools are used to calculate the expected energy production and the expected financial yield [3].

Fluctuating solar resource induces at least daily ramps ups and downs in the solar field, thermal storage unit and usually also in the power producing unit. Due to their daily occurrence, these transient effects have significant impact on the yield. At the same time, they are the most complex part to consider since the chosen operating strategy and individual daily situations affect the realized trajectories. Additional effects are caused due to non-steady irradiation conditions typically induced by clouds. These do not only reduce the available irradiance (which is well mapped by the tools) but additionally cause losses due to required control actions often resulting in partial defocusing. When comparing simulated data with real operational data the transient effects are typically responsible for a large part of the deviations in the magnitude of 5-10 % [4]. Fig. 1 shows an example of the behavior of a real power plant in comparison to the simulated values on three days. Here it can be seen that on the first day with nearly clear sky conditions the simulated values, like temperature, are very similar to the real data. Differences occur in the transient conditions like on day three where variable irradiation conditions are given and the values between real power plant and simulation model show differences.

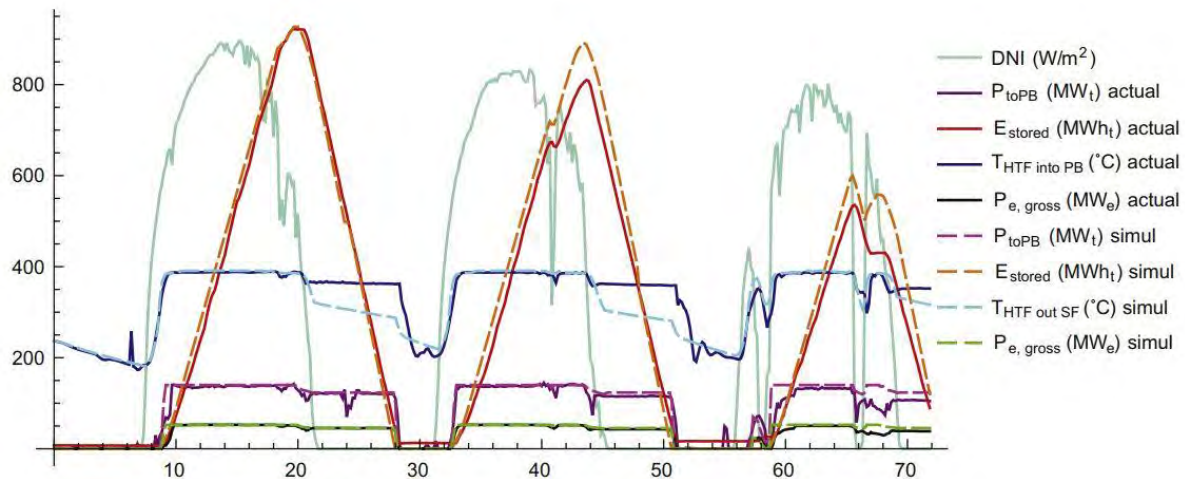


Fig. 1. Comparison of real data with a simulation model on three days. [4]

Detailed modeling of the transient effects is usually not appropriate or possible for feasibility studies. The approach of this work is therefore to develop approaches how transient effects can systematically be included in yield simulation tools by means of parametrized simplified models. In order to optimize the annual yield tools, there are first approaches which extend the steady-state models by the influence of dynamics with the help of parameters [3]. The parameters or characteristics of such models should be derived by automatically analyzing operational data of typical plants. The core of the work is thus to develop a more or less automatic algorithm to identify the impact of transient effects from long time operational data of a plant. The method will be developed and pre-tested by means of the virtual solar field model available at DLR. Real operational data from at least one plant shall then be used to demonstrate the approach. Having such an approach available will help to derive typical transient effect characteristics from a magnitude of plants and thus come one step closer to real conditions in the yield modeling.

[1] F. Schöniger, R. Thonig, G. Resch, J. Lilliestam, Making the sun shine at night: comparing the cost of dispatchable concentrating solar power and photovoltaics with storage, *Energy Sources, Part B: Economics, Planning and Policy*, 16:1 (2021) 55-74

[2] J. Dersch, M. Binder, C. Frantz, S. Giuliano, F. Gross, H. Hasselbach, N. Kaczmarkiewicz, F. Klasing, J. Paucar, T. Polklas, C. Schuhbauer, A. Schweitzer, A. Stryk, D. Többen, CSP-reference power plant "Made in Germany", *AIP Conference Proceedings* 2445, 010001 (2022)

[3] T. Hirsch u. a. *SolarPACES Guideline for Bankable STE Yield Assessment*. IEA Technology Collaboration Programme SolarPACES, 2017

[4] Llorente García Isabel, Álvarez José Luis and Blanco Daniel, Performance model for parabolic trough solar thermal power plants with thermal storage: Comparison to operating plant data, *Solar Energy*, 85 (2011) 2443-2460

Potential applications of CSP technology in high-temperature industrial processes in Chile

Juan Sebastián Zuleta Marin¹, Dr. Werner Platzer¹, Dr. Gregor Bern¹, Dr. Frank Dinter²

¹*Fraunhofer ISE, Institute for Solar Energy Systems, Freiburg im Breisgau, Germany*

²*Center for Solar Energy Technologies, Fraunhofer Chile Research, Santiago, Chile*

juan.sebastian.zuleta.marin@ise-extern.fraunhofer.de

Abstract

Thermal and electrical demands worldwide have dramatically increased because of the population and industrial growth, and fossil fuels are still essential to meet these demands. However, the massive use of fossil fuels has resulted in negative impacts such as climate change, air pollution, and other harmful aspects. As a result, the efforts have been focused on the rapid development of renewable energy to significantly reduce CO₂ emissions. In the last years, solar energy has been considered as an important solution to achieve this goal. For this reason, many countries and research groups have been working on reducing the cost of solar systems, on increasing their thermal and electrical efficiencies, and on looking for new applications where solar energy can have an important impact. The most common application concerning solar energy is photovoltaic (PV) systems, which are characterized by the direct conversion of sunlight to electricity. On the other hand, Concentrated Solar Power (CSP) systems use a combination of mirrors to reflect and concentrate sunlight onto a receiver where a heat transfer fluid is heated up. This energy can be used to spin a turbine or power an engine to produce electricity. It can also be used in a variety of industrial applications such as water desalination, enhanced oil recovery, food processing, chemical production, mineral processing among other applications. Currently, there are four CSP technologies classified in linear receiver technologies (parabolic trough and linear Fresnel) and single point receiver (solar tower and parabolic dish) which can potentially meet thermal and electrical demands in some industrial processes. These technologies can deliver energy in a wide range of temperatures according to the required application which are commonly divided into low-temperature (<100°C), medium-temperature (200 – 400 °C), and high-temperature (>400 °C). Another important way to reduce global emissions is by means of Carbon Capture Technology (CCT) which basically prevent CO₂ from being released into the atmosphere. Currently, there are three different CCT technologies named: pre-combustion, post-combustion, and oxy-fuel combustion among these available technologies, post-combustion technology with chemical absorption with liquid solvents is the most mature technology. In fact, chemical absorption with amine solutions has been extensively used and has reached commercial scale demonstration in coal fire power plants. To achieve carbon neutrality by 2050, it is expected that the role of

CCT will be important especially in those industries where thermal and electrical demands are high and therefore a significant amount of fuel is required. After capture CO_2 , it can either be stored or used to produce fuels, chemicals, and materials. Power-to-gas technology (PtG) is a form of CO_2 utilization, in which Synthetic Natural Gas (SNG), rich in methane (CH_4), is produced from the reaction of CO_2 with hydrogen (H_2) previously obtained by water electrolysis. Concerning the potential of Chile for solar energy, it has been identified a great potential for the integration of solar energy applications mainly due to the high annual irradiation values found across the country (1,800 – 3,600 kWh/m^2 per year), especially in the north where the irradiation is higher than 2,500 kWh/m^2 per year. In this regard, the primary purpose of this research is to define the potential opportunities and the main barriers associated with the implementation of CSP technologies in some Chilean industrial processes which are conducted at high temperature (above 400 °C) such as some processes in the chain production of cement, cooper, and steel industries. To do so, it will be analyzed and simulated some CSP layouts based on criteria selection including solar irradiance, water availability, annual thermal demands, range of working temperature, availability of Heat Transfer Fluid (HTF), weather profile, operation time, economic aspects, land availability, access to raw material needed for the operation of the CSP plant, type of industry, among other aspects. In addition, it will be also studied the potential of CO_2 capture technologies for producing CH_4 after obtaining H_2 from an electrolysis process. The proposed CSP layouts will be evaluated through an economic analysis and sensitivity analysis to determine new opportunities for savings and optimize the layouts studied.

Application of AI methods to improve Operation and maintenance of CSP power plants

Thomas Kraft, Dr. Thomas Fluri, Dr. Werner Platzer

Fraunhofer ISE, Insitut for Solar Energy Systems, Freiburg im Breisgau, Germany

Mail: Thomas.kraft@ise.fraunhofer.de.

In today's society, large amounts of data are collected for the operation of solar power plants and used to regulate or control individual components. The measurement technology required for data collection in the form of cost-effective sensors is available on an industrial scale. However, there is often a lack of medium- and long-term use of this data to improve operation and maintenance at the power plant level. On one hand, this requires the acquisition of this data to the operating personnel, and on the other hand, the evaluation by means of machine control algorithms. In addition to operation, machine learning or artificial intelligence is not used often for maintenance. Recently published research results from the literature show that machine learning algorithms such as artificial neural networks (ANN) are suitable for recording the main influencing factors of a parabolic trough collector (exemplarily specifically the outlet temperature) and thus contributing to the optimization of operation[1]. The quality of the optimization depends significantly on the type of machine learning algorithm. For example, the ANN with the variant of Levenberge Marquard (LM) in particular is attributed to significant improvements of the CSP thermal efficiency [2]. Further studies suggest that the applicability and accuracy of machine learning models depends heavily on the investigated components of the system (solar field, heat exchangers, pumps) [2]. Although the first studies on machine learning in the field of CSP were presented more than 10 years ago, use of the various machine learning algorithms in large-scale and combined power plant processes and maintenance methods is not often seen in practice. Additionally in literature, the optimization of CSP through the use of AI receives little attention.

The aim of the planned doctoral thesis is to improve the power plant operation of solar thermal power plants on the basis of machine learning algorithms in such a way that the competitiveness of CSP against other power plant technologies is strengthened on a scientific basis under practical relevance of at least one real plant. The optimization of both comprehensive operation and maintenance data will be evaluated through various AI models as well as investigating which methods (e.g. neural networks, decision-trees, analytical models) are best suited for this purpose. Additionally, a digital twin will be modelled after an operational CSP plant where the resulting digital twin simulation data will be calibrated against

the operational power plant data. These results obtained will be validated and recommendations for action for operation and maintenance are to be given. The findings will also be compared and discussed with previous results in the literature.

Possible questions of the doctorate, which can also be discussed in the context of this colloquium, are:

- Is machine learning in the field of CSP fundamentally suitable for achieving better results than with physical models? (When? How much data is needed? More concretely, the following will be considered:
 - Over what period of time are data collections from the current operation necessary in order to predict the outlet temperature of individual loops versus currently used physical models?
 - Which machine learning algorithms are best suited to improve the operation of solar power plants with reasonable computing effort?
 - How much can the efficiency of the solar thermal field be increased by using machine learning algorithms?
 - To what extent can loop balancing be improved by more accurate temperature prediction using ANN with the variant of Levenberge Marquard (LM)?
- In what way should the data collection be carried out as far as possible in order to obtain the most relevant data with little time and economic effort?
 - To what extent can the prediction accuracy using ML be improved by changing the data collection (number/location of sensors)?
 - Which maintenance strategy proves to be optimal when using machine learning algorithms?

[1] M. Cervantes-Bobadilla, J.A. Hernandez-Perez, D. Juarez-Romero, A. Bassam, J.García-Morales, A. Huicochea, O.A. Jaramillo, Journal of the Brazilian Society of Mechanical Sciences and Engineering, (2021) 43 :176

[2] I. Muñoz, F. Cortés, A. Crespo, M. Ibarra, AIP Conference Proceedings 2126, 170008 (2019)

Evaluation of equipment for outdoor reflector measurements in CSP solar fields

Johannes Wette¹, Florian Sutter², Aránzazu Fernández-García¹

¹CIEMAT Plataforma Solar de Almería, Ctra. Senés Km. 4, P.O. Box 22, E04200, Tabernas, Almería (Spain), johannes.wette@psa.es

²DLR, German Aerospace Center, Institute of Solar Research, Paseo de Almería 73, 2°, E04001, Almería (Spain)

The reflectance of the solar field mirrors in concentrated solar power (CSP) plants is one of the key parameters determining the field's optical efficiency. The high initial reflectance of commercial mirror materials during operation is prone to changes due to permanent degradation or removable soiling. The correct measurement of the most significant parameter for the optical efficiency, the solar-weighted near-normal sun-conic reflectance [1], is challenging and nowadays can only be performed by specialized laboratories. Regular in-field measurements of the reflectance, to evaluate possible degradation and soiling, are usually performed with commercially available reflectometers, with different characteristics and which all measure different reflectance parameters [2]. So far there is still a lack of data on the comparison of all the available reflectometers on the market to evaluate their suitability for significant measurements of reflectance [3, 4]. For this work, all commonly used devices in the CSP sector were available for a laboratory measurement campaign on different types of solar reflector materials and a comparison between them.

The devices were used to measure a series of different solar reflector materials. The reflectors were chosen to present a variety of reflectance ranges, as well as reflectors of high and low specularity. Among the measured reflector types were: commercial and experimental glass mirrors of different glass thickness, aluminum reflectors and special UV mirrors. At least three measurements were performed on small samples of around 10x10 cm² and the mean values were calculated. The devices measure at one or several specific wavelengths λ or cover more or less broad λ -ranges. All of the devices are able to measure the specular reflectance at one or several acceptance angles φ and some in addition give the hemispherical values. Furthermore, data was compared to measurements of the hemispherical reflectance, performed with a Perkin Elmer (PE) Lambda 1050 spectrophotometer. In the results, the spectral data of the reflectance is compared for the different devices.

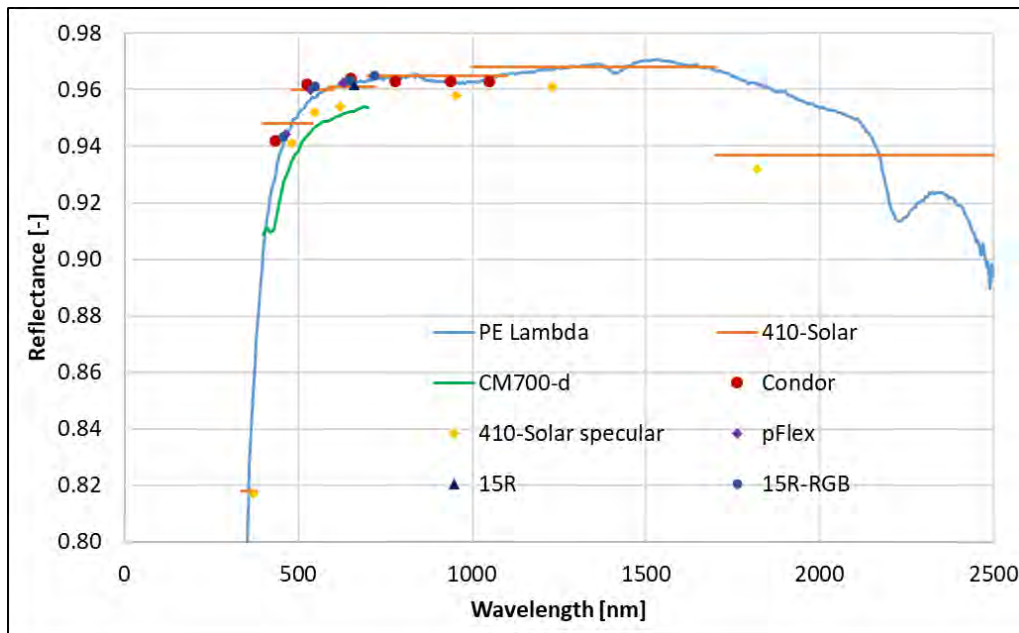


Fig. 2: Reflectance spectra of 2 mm glass mirror measured with different devices.

As an example in Fig. 1, the spectral data of all devices is presented for a 2 mm silvered-glass mirror in the initial state. This type of reflector usually shows very high specularity, which is confirmed by very good agreement between the hemispherical measurements with the PE (blue line) and the specular measurements with the D&S 15-R reflectometer at 660 nm. In general, agreement for the different devices is good and differences are mainly detected depending on the acceptance angle of the respective devices. Detailed results will be presented also for degraded and less specular reflector samples and issues with certain reflectometers will be discussed. The here presented laboratory campaign serves as a preliminary campaign for a more extended outdoor campaign.

[1] M. Montecchi, AIP SolarPACES conference proceedings, Cape Town, South Africa, (2015).

[2] A. Fernández-García, A., F. Sutter, L. Martínez-Arcos, C. Sansom, F. Wolfertstetter, C. Delord, *Solar Energy Materials and Solar Cells*, 167, 28–52 (2017).

[3] J.S. Crawford, J. Stewart, and J.A. Pérez-Ullivarri, *SolarPACES conference proceedings*, Marrakech, Morocco, (2012).

[4] C. Sansom, A. Fernández-García, P. King, F. Sutter, and A. García-Segura, *Solar Energy* 155, 496 (2017).

Characterizations and tests on the new Fresnel solar furnace testing platform at the Plataforma Solar de Almeria

N. Estremera-Pedriza, J. Fernández-Reche

CIEMAT-Plataforma Solar de Almería. noelia.estremera@psa.es

Currently, we are seeing that having energy independence from other countries is a necessity, and solar thermal power plants (in particular tower plants) can help in this, as they have great potential to generate electricity. However, solar thermal energy needs to become even more efficient, economical and durable. This can be achieved not only by reducing costs, but also by increasing the temperature at the receiver and increasing solar concentration. But the materials that make up the metallic tubes of the receiver towers in particular have high demands: they must be able to achieve high fluxes of concentrated solar radiation ($>1 \text{ MW/m}^2$) and high temperatures ($>800^\circ\text{C}$). Therefore, an optical and thermal study on the aging of these materials will be carried out to estimate their durability. This will be carried out in the new solar furnace of the Plataforma Solar de Almeria (PSA).

Continuing with the fine-tuning of this new solar furnace installation, characterizations were made of the variable transmissivity screen and 6 mirrors available to filter the wavelengths of the solar spectrum on the material, each with a different selective reflectance.

The characterization of the variable transmissivity screen was carried out by varying the state between opaque and translucent, and measuring luminance before and after the screen with a KAINOS MAVOLUX digital luxmeter. As a result, an approximate transmissivity of 0.7 in opaque state and 0.8 in translucent state was obtained.

On the other hand, Table I shows the spectral characteristics and specifications of the selective spectral reflectance mirrors [1], as well as the percentage of solar radiation reflected by them with respect to the standard AM1.5 solar spectrum, ASTM G173-03 [2].

Table I. Mirrors, wavelength bands and their specifications

Nº Mirror	Band (nm)	Irradiance of solar spectrum (%)	Specifications
1	450 – 10.000	96,7	50 mm diameter. Protected silver
2	250 – 700	87,7	50 mm dia. UV Enhanced Aluminum
3	700 – 10.000	82,3	50 mm diameter. Protected gold
4	450 – 650	91,3	50 mm dia. Enhanced Aluminum,
5	400 – 700	90,9	Espejo 73 x 116 mm, mirror 4-6 λ
6	400 – 1.125	44,1	Espejo 45° AOI, 101 x 127mm

The mirrors of most interest from the spectral point of view are mirrors n°3 and n°6 because, as can be seen in Figure 1, mirror n°3 (red curve) significantly reduces the ultraviolet and visible wavelengths, while keeping the infrared area of the solar spectrum unchanged. On the other hand, mirror n°6 (blue curve) acts as a bandpass filter between the ultraviolet and near infrared. Therefore, they are the mirrors that filter the solar spectrum in wavelengths below 625 nm. As these wavelengths are the more energetic ones with more potential to photooxidize the materials [3]. In addition, as can be seen in Table I, they are the mirrors with the lowest percentage of reflected irradiance so, the mirrors that reflect less energy. It's very likely that these mirrors significantly modify the behavior of the solar radiation on the material modifying the microstructure.

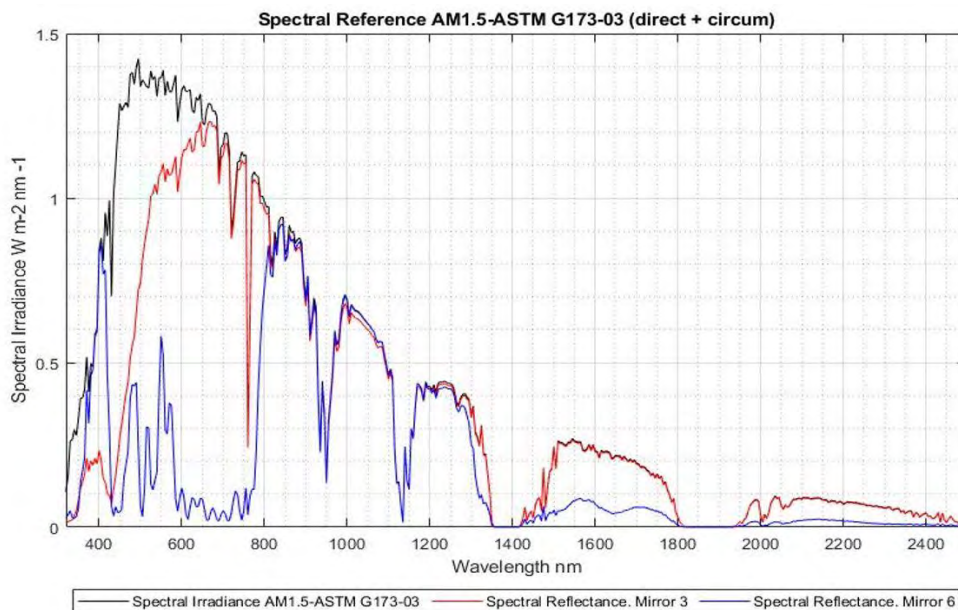


Fig.1. Spectral reflectance of mirrors n°3 and n°6 with respect to irradiance [2]

Finally, the solar furnace is ready for operation, we will start testing on the 625 Nickel alloy as it is the most used in solar tower receivers (metal tubes), these tests will be performed exposing the solar radiation reflected with these mirrors on the material to check the behavior in these cases, to find out if there are dependences between the wavelengths of the solar spectrum and the aging of the material.

Acknowledgment

The authors thank the Ministry of Science, Innovation and Universities (Spain) for the funding received in the SOLTERMIN project (Reference ENE2017-83973-R).

References

- [1] Edmund Optics Europe
https://www.edmundoptics.eu/?gclid=EA1alQobChMIPmE6t7o9gIVCJ7VCh31Cg66EAAYASAAEgJ5qfD_BwE. Last access March 30, 2022.
- [2] NREL Transforming Energy
 Reference Air Mass 1.5 Spectra (AM 1.5, ASTM G173-03 Reference Spectra)
<https://www.nrel.gov/grid/solar-resource/spectra-am1.5.html>. Last access June 10, 2022.
- [3] E. Setien, J. Fernández-Reche, M. Álvarez-de-Lara, and M. J. Ariza, "Experimental system for long term aging of highly irradiated tube type receivers," *Sol. Energy*, vol. 105, pp. 303–313, 2014, July, 2014, doi: 10.1016/j.solener.2014.04.004.

Approach for modelling the thermal performance of a Linear Fresnel Collector with a Trapezoidal Cavity Multi-tube Receiver

Sergio Alcalde-Morales¹, Loreto Valenzuela¹, J.-J. Serrano-Aguilera²

¹CIEMAT-Plataforma Solar de Almería, Crta. Senes, km 4.5, 04200 (Almería), Spain;

e-mail: sergio.alcalde@psa.es

²Universidad de Málaga, Escuela de Ingenierías Industriales, Campus de Teatinos s/n, 29071, Málaga, Spain.

1. Introduction

The aim of this work is to contribute to the thermal analysis of linear Fresnel solar collectors (LFC) with cavity receivers using a multi-tube absorber. The work is being applied to a whole innovative LFC [1], which is currently under commissioning at Plataforma Solar de Almería (PSA).

Regarding the thermal analysis of parabolic-trough collector (PTC) systems, 2-D models have been taken into account in many works available in literature [2-3]. Also, 3-D models have been proposed [4-5], but by means of CFD software, what implies a big computational cost. In [6] a 3-D model is proposed, using a 1-D model for modelling the thermal behavior of the heat transfer fluid (HTF). In the present thesis, a similar coupling between the heat conduction problem in the absorber wall and the HTF domain is applied for the thermal modelling of the LFC system studied.

2. Methodology

In order to solve this problem, heat losses correlations from a previous work will be used. These correlations describe the heat losses from the absorber tubes as function of their outer temperature. The heat diffusion across the absorber wall is solved by means of a new semi-analytically approach (2D-model) by the method of separation of variables, whereas HTF PDE equations are solved numerically by the method of characteristics (1D-model).

Heat flux is given by the heat equation (eq. 1), which is solved knowing net heat flux through exterior surfaces of the tubes (eqs. 2), where q_{sun} is the radiation incident on the tubes as a result of the incidence of sunlight on the mirrors of the LFC, obtained by ray-tracing using Tonatiuh (figure 1). The heat flow q_{out} is got by heat loss correlations. Temperature $T(t, r_{in}, \phi)$ is known too, given by a previous resolution of the Navier-Stokes equations (eqs. 3) for HTF, where mass flux (G) is known and Q_{HTF} is the integral of the heat flux received by the fluid through the tubes by conduction. Temperature $T(t, 0)$ and pressure $p(t, 0)$ are known too.

$$\frac{1}{r} \frac{\partial}{\partial r} \left(r \frac{\partial T}{\partial r} \right) + \frac{1}{r^2} \frac{\partial^2 T}{\partial \phi^2} = \frac{\rho C_p}{k} \frac{\partial T}{\partial t} \quad (1)$$

$$k \frac{\partial T_{out}}{\partial r} = q_{sun} - q_{out} \quad (2.a)$$

$$k \frac{\partial T_{in}}{\partial r} = q_{HTF} \quad (2.b)$$

$$\frac{\partial \rho}{\partial t} + \frac{\partial G}{\partial z} = 0 \quad (3.a)$$

$$\frac{\partial G}{\partial t} + \frac{\partial}{\partial z} \left(\frac{G^2}{\rho} \right) + \frac{\partial p_{fric}}{\partial z} + \rho g \sin(\theta) + \frac{\partial p}{\partial z} = 0 \quad (3.b)$$

$$\rho \frac{\partial h}{\partial t} + G \frac{\partial h}{\partial z} = Q_{HTF} \quad (3.c)$$

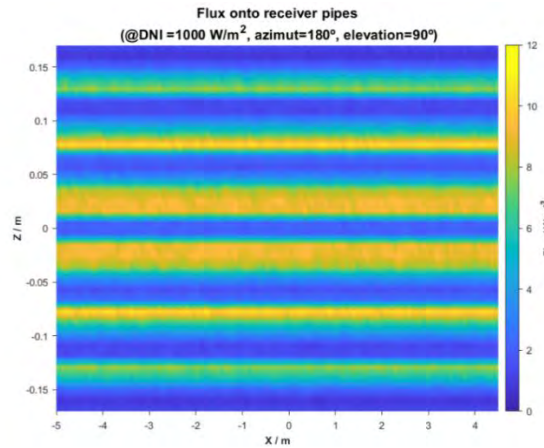


Figure 1. Example of 2D heat flux map onto the outer surface of the 6 tubes of the LFC receiver analyzed.

Due to q_{out} is not known a priori, an iterative procedure must be carried out: heat flux Q_{HTF} is supposed. Applying boundary condition for HTF, $T(t, z)$ is obtained. $T(t, z) = T(t, r_0, \phi, z)$ is used as the boundary condition for the heat equation, and using eqs. 2, temperature field $T(t, r, \phi, z)$ is obtained. Using heat losses correlation, q_{out} is obtained, and Q_{HTF} is recalculated. The iterative process continues until convergence. The results obtained in simulation will then be compared to the experimental results.

Acknowledgment: Authors thanks Spanish government for funding SOLTERMIN project (ENE2017-83973-R).

[1] Pulido D, Valenzuela L, Serrano JJ and Fernández A. Renew Energy 2019;131:1089-106

[2] Tao Y, He Y. Solar Energy 2010;84(10):1863–72.

[3] Hachicha A, Rodríguez I, Capdevila R, Oliva A. Appl Energy 2013;111(0):581–92.

[4] Cheng Z, He Y, Xiao J, Tao Y, Xu R. Int Commun Heat Mass Transfer 2010;37(7):782–7.

[5] Cheng Z, He Y, Cui F, Xu R, Tao Y. Sol Energy 2012;86(6):1770–84.

[6] Serrano-Aguilera JJ, Valenzuela L and Parras L. Applied Energy 2014;132:370-382.

Deep learning inversion of a raytracer

Jan Lewen^{1,2,3}, Mathias Kuhl^{1,2}, Max Pargmann¹, Medi Cherti², Jenia Jitsev², Daniel Maldonado Quinto¹

¹ German Aerospace Center (DLR), Institute of Solar Research, Cologne, Germany

² Forschungszentrum Jülich (FZJ), Jülich Supercomputing Center, Jülich, Germany

³jan.lewen@dlr.de

Concentrating solar power plants (CSP) play an important role in the world's transition to a sustainable energy supply due to their cost-effective energy storage systems and hence their ability to deliver power on demand even in the absence of solar radiation. A key variable for safe and optimal control of the power plant is the concentrated flux density distribution on the receiver. Unfortunately, the exact surface profile of the heliostat, including canting and mirror error, is difficult to measure for a large number of operating heliostats. Therefore, control systems that use flux density predictions from ray tracers use ideal surface assumptions. This leads to inaccurate predictions that compromise safety and efficient operations.

This work uses deep learning methods to invert a physical ray tracer and hence to predict the exact surface of a heliostat, on the basis of its caused flux densities under different sun positions. The method should be easy incorporable in the regular operation of the power plant. Hence, for training the network and the following surface prediction, the only real data we use are recorded during the regular operation, as the calibration measurements delivering flux density data. In this talk we will present a model, that is capable of learning to predict simulated surfaces on the basis of the flux densities generated by the surfaces. [1]

Challenging is the scarce availability of surface data for training the model as well as the strongly ill-posed, underdetermined nature of this inverse problem. To handle those problems, we elaborate how training with artificially generated data from ray tracer can be used further on for transferring pre-trained models to small volumes of real data when using sufficiently large and diverse artificial datasets for pre-training.



A suitable deep neural network architecture needs to handle input data of different kind (multiple images and scalar data) to learn a mapping from flux density space and sun positions to a cartesian representation of the surface. We found that adaptive instance normalization (AdaIN) is a well working approach for combining the different input data. We make use of a compact latent representation of the heliostat properties, which entails hidden variables of the surface prediction problem that we learn to infer from flux density and sun position data. From the latent heliostat space, we decode and finally generate cartesian representation of the full surface.

In a final step one can replace the ideal surface assumptions in the control systems that use flux density predictions from ray tracers with the surface predictions and hence reduce the modelling error.

GAN-based Calculation of Concentrated Radiation on Solar Tower Receivers [1] Lewen, Kuhl, Pargmann, Cherti, Jitsev, Maldonado Quinto, Helmholtz AI conference, Dresden, Germany, 2022

This work is funded by the Helmholtz association and is part of the Helmholtz Artificial Intelligence Cooperation Unit (HAICU)

A purely data-driven deep learning digital twin approach for a heliostat field for flux density predictions

Mathias Kuhl^{1,2,3}, Jan Lewen^{2,3}, Max Pargmann², Mehdi Cherti³, Jenia Jitsev³,
Daniel Maldonado Quinto²

¹mathias.kuhl@dlr.de

²German Aerospace Center (DLR), Institute of Solar Research, Cologne, Germany

³Forschungszentrum Jülich (FZJ), Jülich Supercomputing Centre, Jülich, Germany

Controlling the flux density distribution on the receiver in solar tower power plants is crucial to guaranteeing the durability of components and maximizing the power plant's performance. Therefore, it is crucial to have a precise prediction of the current and future flux densities. However, obtaining this flux density is particularly challenging, because the unique mirror surface deformations of each heliostat affect the resulting flux density strongly. Although there are raytracers that may predict a flux density with analytical calculations, such a method falls short of accurately representing reality by assuming an ideal surface. This includes, that common methods for measuring the surface deformations are either inaccurate, complicated, or expensive.

We present a novel purely data driven AI based digital twin approach to predict the flux density distribution on the receiver, which is capable to include heliostat specific errors, without having to measure the heliostats surface. The model is trained with measurements of flux density distributions of the individual heliostats, which are obtained during the calibration process. From those measurements a latent vector for each heliostat is inferred, which contains a compact representation of the entire heliostat state including surface deformations. This heliostat model is latent, because its variables are not directly observed, but are causes inferred from observed flux density data by using an inverse mapping learned from a dataset of measured flux densities. The inverse mapping is learned from data without using strong assumptions on heliostats physics and thus any physics-informed regularization. These inferred latent variables are input for a generative neural network, which is able to predict the flux densities at different sun positions.

We present the digital twin model architecture, as well as the training procedure of the purely data-driven model, and show first results on artificial and also real data.

Geometric optimization of linear Fresnel collectors for solar thermal electricity

André Vitor Santos, Diogo Canavarro.

University of Évora – Renewable Energy Chair (avas@uevora.pt).

The optimum geometric design of a Linear Fresnel Collector (LFC) is not a simple problem. Many works have been published on this subject, although no convergence about optimum (dimensionless) parameters has been found. On the other hand, some important lessons can be derived from the literature: ray-tracing constraints the optimization due to its time-consuming simulations [1,2]; the main issue is related to optical performance, but it is also essential to consider economic parameters to evaluate whether a solution is cost-effective or not [1,3]; the objective functions should be carefully defined to avoid trivial optimum (e.g., the ones with a large number of tiny mirrors [1] or with a small number of large mirrors [4]).

This Ph.D. research proposes a study to overcome these issues and answer two questions: (1) What are the optimum ratios between receiver height and primary field width? (2) What (dimensionless) geometric parameters define the optimum primary field configurations (widths, shifts, and curvatures)? To achieve such goals, it considers a multi-objective approach, where a cone-optics method computes the optical performance (a fast computation enables the comparison of objective functions to avoid trivial solutions), and an economic model relates geometric parameters with a measure of cost [1]. Furthermore, it considers evolutionary algorithms as the optimum search heuristic since such stochastic population-based methods are a proven strategy to determine the Pareto solutions [5].

Some works were already done related to the steps of this research. First, a bi-axial analytical optical method for LFCs with a flat receiver was developed to replace ray-tracing simulations [6]. Although a flat receiver is unusual, it can be interpreted as the aperture of a secondary optic. Its computations of annual energetic yields presented an error lower than 1% regarding the ray-tracing results for factorized models – a good agreement between the methods.

Then, a geometric optimization study based on genetic algorithms was conducted for an LFC with a flat receiver, uniform width, and uniform shift between neighbor mirrors [4]. It aimed to optimize variables to maximize the annual optical efficiency. The definition of such an objective function resulted in a trivial solution – a small number of large mirrors – since it is a relative measure and there was no other objective to push the optimum to different geometries.

The current research is related to the curvature design of primary mirrors. Different designs have been proposed but were never confronted all at once. Some first results of annual optical

efficiency indicate a slight difference between highest and lowest values: up to only 1.78%, which states that the designs are virtually identical. However, this evidence needs further discussion regarding the tolerance to optical errors, i.e., the acceptance angles.

The following main steps are related to the definition and implementation of objective functions and an evolutionary algorithm (such as genetic algorithms, evolutionary strategy, and particle swarm optimization) able to handle the specificities of the problem.

The development of the ALFR-Alentejo project [7] in the Renewable Energy Chair (REC) of the University of Évora moved the ongoing LFC design research beyond the secondary optic to include the primary field. It is expected that this Ph.D. research will enhance the perception of the relations between geometric parameters, optical performance, and costs to improve the understanding of the cost-benefit perspectives of this technology – activities closely connected to Task 10.2.3 of the SFERA-III project on the testing of LFC collectors.

References

- [1] M.A. Moghimi, K.J. Craig, J.P. Meyer, Simulation-based optimisation of a linear Fresnel collector mirror field and receiver for optical, thermal and economic performance, *Solar Energy*. 153 (2017) 655–678. doi:10.1016/J.SOLENER.2017.06.001.
- [2] Z.D. Cheng, X.R. Zhao, Y.L. He, Y. Qiu, A novel optical optimization model for linear Fresnel reflector concentrators, *Renewable Energy*. 129 (2018) 486–499. doi:10.1016/j.renene.2018.06.019.
- [3] P. Boito, R. Grena, Optimization of the geometry of Fresnel linear collectors, *Solar Energy*. 135 (2016) 479–486. doi:10.1016/j.solener.2016.05.060.
- [4] S.C. Costa, A. Santos, D. Canavarro, I. Malico, F. Janeiro, Optimization of Linear Fresnel Reflector Solar Collectors Using a Genetic Algorithm, in: *5th International Conference on Numerical and Symbolic Computation: Developments and Applications, SYMCOMP 2021, Évora, 2021*: pp. 163–172. https://www.eccomas.org/wp-content/uploads/sites/15/2021/04/symcomp2021_proceedings.pdf.
- [5] K. Deb, *Multi-Objective Optimization using Evolutionary Algorithms*, John Wiley & Sons, New York, 2001.
- [6] A.V. Santos, D. Canavarro, P. Horta, M. Collares-Pereira, An analytical method for the optical analysis of Linear Fresnel Reflectors with a flat receiver, *Solar Energy*. 227 (2021) 203–216. doi:10.1016/j.solener.2021.08.085.
- [7] D. Canavarro, M. Collares-Pereira, A. Santos, G. Delgado, P. Horta, ALFR-ALENTEJO: DEMONSTRAÇÃO EXPERIMENTAL DE UM PROTÓTIPO ADVANCED LINEAR FRESNEL REFLECTOR EM ÉVORA, in: *CIES2020: Livro de Comunicações Do XVII Congresso Ibérico e XIII Congresso Ibero-Americano de Energia Solar, Lisboa, 2020*: pp. 1–7. <https://doi.org/10.34637/cies2020.1.2018>.

Numerical Simulation of Pressure Drop in Wire Mesh Absorbers with Fixed Porosity

Daniel Sanchez-Señoran^{1,2}, M. Reyes-Belmonte², J. Fernandez-Reche³ and A. Ávila-Marín¹

¹ CIEMAT – Plataforma Solar de Almería, Avda. Complutense 40, Madrid E-28040, Spain

² Rey Juan Carlos University (ESCET), C/ Tulipan s/n, Mostoles-Madrid E-28933, Spain

³ CIEMAT – Plataforma Solar de Almería, P.O. Box 22, Tabernas-Almería E-04200, Spain.

1. Introduction

Heat transfer coefficient and hydrodynamic performance are the main properties to evaluate the efficiency of a volumetric absorber. Hydrodynamic performance is based on pressure drop and air flow instabilities, which should be minimized [1] in order to improve the efficiency of the volumetric absorber. The main materials used in volumetric absorbers are metals and ceramics [2]. There are some studies of the pressure drop for porous media especially foams [3], however, it exists a lack of literature when talking about numerical simulation of the pressure drop behavior for wire mesh volumetric absorbers in concentrated solar power.

In this work, numerical simulations of pressure drop behavior will be evaluated in three different volumetric absorbers and a velocity ranging from 0.5 to 5 m/s. These absorbers will have fixed the porosity, 80%, and wire diameter will be varied as follows: 0.1, 0.4 and 0.7 mm.

2. Geometrical properties

There are two highlighted parameters that define wire mesh screens [4], the wire diameter, d (mm) and, the mesh count, M (mm^{-1}). According to these parameters, different geometrical properties could be inferred, such as volumetric for single screen and for staggered stack porosity (ϕ_{SS} and ϕ_{ST}), specific surface area (a_v) as it is shown in Table 1:

Case	Wire diameter, d (mm)	Mesh count M (mm^{-1})	Single screen porosity, ϕ_{SS} (%)	Staggered stack porosity, ϕ_{ST} (%)	Specific surface area, a_v (m^{-1})
# 1	0.7	0.35	80	64.3	2,031
# 2	0.4	0.61	80	64.4	3,548
# 3	0.1	2.44	80	63.9	14,001

Table 1. Properties of the volumetric absorber with stagger stack wire meshes.

This work analyzes the pressure drop in two different stagger stack arrangements, Fig. 1. a) is the characteristic geometrical arrangement used for the numerical simulations of the heat transfer coefficient, and Fig. 1. b) is the arrangement used in some experimental literature [4]:



Fig. 1. Studied arrangements for pressure drop: (a) Rectangular and (b) Circular.

3. Numerical simulation and results

The commercial CFD software STARCCM+ v16.02.009 is used to build the tortuous and detailed 3D geometries studied in this work. In order to study the pressure drop, next assumptions are assumed:

- Steady state and laminar flow conditions.
- Fluid is defined as a constant density due to this study is performed at 300K.
- The lateral walls of the 3D body have been under study and have been defined firstly as a symmetry plane and secondly as a wall.

The results will present a comparison of the pressure drop between the different cases (#1, #2, #3). A comparison between the two stagger stack arrangements (Fig. 1. a, and Fig. 1. b), and for the two lateral walls boundary conditions presented before. Fig. 2 depicts the main results for case #3, in which is observed that there are small differences between the arrangements and boundary's modifications, however, the higher the velocities, the bigger the differences between boundary's modifications. Also, it is noticeable the difference between the arrangements for the wall boundary at 5 m/s.

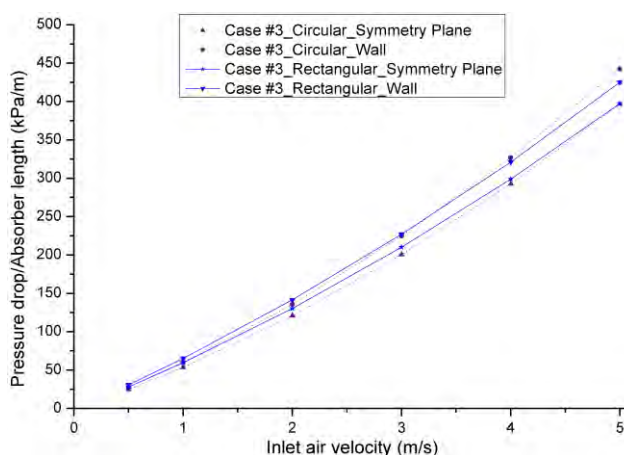


Fig. 2. Pressure drop along the mesh length for each inlet air velocity in case #3 and both arrangements.

4. References

- [1] F. Gomez-Garcia. Renewable and Sustainable Energy Reviews, 57(2016), 648-658.
- [2] A.L. Ávila-Marín. Solar Energy, 85(2011), 891-910.
- [3] Z. Wu. Applied Energy, 87(2010), 504-513.
- [4] A.L. Avila-Marin. Renewable Energy, 122(2018), 339-353.
- [5] M. Becker. Solar Energy, 80(2006), 1241-1248.

Optimization of Spinel Absorber Coatings for CSP Particle Receivers

Meryem Farchado¹, Raúl Tordesillas², Gema San Vicente¹, Nuria Germán¹ and Ángel Morales¹

¹ CIEMAT-PSA. Materials for Concentrating Solar Thermal Technologies Unit.

Avda. Complutense 40, Madrid 28040 Spain, meryem.farchado@ciemat.es

² Universidad Autónoma de Madrid. C. Universitaria de Cantoblanco, Madrid 28049 Spain.

1. Introduction

The energy crisis of recent decades has greatly inspired the search for alternatives to traditional fossil fuels, among which solar energy stands out as an important candidate due to its abundance and respect for the environment. Since high operating temperature leads to higher power conversion efficiency and lower cost, there is an increasing interest in improving the current commercial plants of concentrating solar power systems (CSP). This improvement focuses on designing systems that can reach higher temperatures (390°C for thermo-oil and 560°C for molten salt) [1]. Nowadays, solid particles are potential candidates to be used as receiver [2] in CSP plants to increase their operating temperature and efficiency as well as thermal storage medium for reducing the complexity and costs of the system. In this novel concept, the solar receiver is constituted by solid particles that are responsible of the direct solar radiation absorption. Hence, these solid materials require withstanding high temperature oxidation and erosion [3]. Within the HORIZON 2020 COMPASsCO2 project, the integration of CSP particle systems into a highly efficient-CO2 Brayton power cycles for electricity production is pursued. Therefore, one of the main tasks focuses on the design, development and test high performance particles for CSP receivers. To this end, different particles developed by Saint-Gobain have been coated with new developed coatings in order to ensure good optical properties and study their high temperatures and abrasion resistance.

2. Experimental and Results

Four porous “state-of-the-art” particles developed by Saint Gobain (BauxLite/BL, Sintered Bauxite/SB and Interprop/IP) [4], were coated with black spinel solutions by dip-coating technique in order to improve their optical and mechanical properties. The influence of depositing consecutive spinel-layers on particles and their curing temperature on the solar absorptance (α_s) value has been analysed. The solid particles have been coated with a maximum of four spinel layers and were sintered in two different ways as specified in Table 1. As can be seen in Figure 3, the coated solid particles sintered according the method 2 registered higher α_s values than the sintered following the method 1. Therefore, the method 2 was selected as the optimal heat treatment for performing the succeeding studies.

Methods of heat treatment	
Method 1	Method 2
Each deposited layer of spinel was sintered at 600 °C, 1 h. After the fourth layer, the particles were heated at 1000 °C, 2 h.	Each deposited layer of spinel was sintered at 1000 °C, 2 h.

Table 2. Description of the two methods used for sintering the spinel coatings.

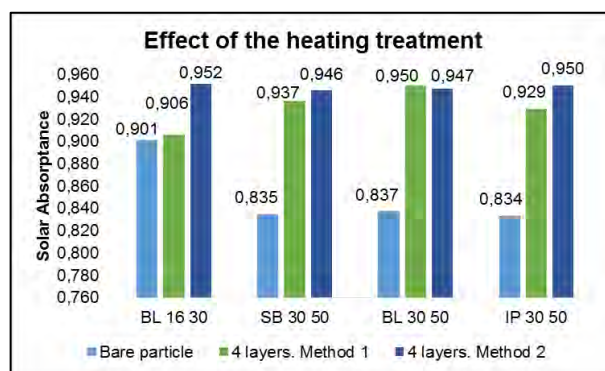


Figure 3. Effect of the spinel sintering on the α_s for the porous state-of-the-art particles tested.

A greater concentrated spinel solution has been tested in BL 30/50 particles in order to optimize the spinel deposition process and thus reduce the number of layers needed. As the concentrated solution of spinel has a higher viscosity, clear differences between not applying and applying one /two spinel layers have been noticed. However, between applying two or three layers, the improvement in solar absorptance was no as drastic. The BL 30/50 particles coated with three spinel-layers and sintered at 1000 °C for 2 hours registered a α_s of 0.955.

Additional tests have been performed depositing a new spinel solution composition (porous solution) on a new solid particle candidate (Gen3). The dense granulated Gen3 particles, developed by Saint-Gobain, were used given its higher hardness and heat capacity in comparison with the four porous “state of-the-art” particles used in the first experiments. A comparative study has been carried out between coating Gen3 particles with four layers of pristine spinel (α_s of 0.942) or four layers of porous spinel (α_s of 0.970). Their respective optical properties and resistance to abrasion have been studied. Up to now, 1000 cycles of 100cm/min have been carried out in a TABER oscillating tester mod. 6160. No losses in the solar absorptance value have been noticed for any of the two samples analysed. Further cycles of degradation by erosion are going to be tested.

References

- [1] A. Palacios, A. Calderón, C. Barreneche, J. Bertomeu, M. Segarra, A.I. Fernández, Solar Energy Materials and Solar Cells, 201 (2019) 110088.
- [2] C.K. Ho, Applied Thermal Engineering, 109 (2016) 958-969.
- [3] T. Galiullin, B. Gobereit, D. Naumenko, R. Buck, L. Amsbeck, M. Neises-von Puttkamer, W.J. Quadackers, Solar Energy, 188 (2019) 883-889.
- [4] S.M.a.I. Amirouche, (2021).

Numerical simulation of Improved Design for an Integrated Receiver and Storage system for CSP applications

Christos Tengeris, Marios C Georgiou, Costas N. Papanicolas

The Cyprus Institute (Cyl), c.tengeris@cyi.ac.cy

The present work presents our research centered around the study and optimization of the receiver and storage component of a small scale Concentrated Solar Power (CSP) power generation and desalination facility. This project aims to improve upon of the successful design, implementation and testing of a novel integrated receiver, named Integrated Storage Receiver (iSTORE) at the PROTEAS (Platform for Research, Observation, and TEchnological Applications in Solar Energy) Facility of the Cyprus Institute[1,2]. This follow up project is devoted to the characterization through simulation of the heat transfer properties of the improved iSTORE design as well the assessment of first and second law efficiencies of the receiver-tank system. In the study we are utilizing the rich results derived from the first generation system[3] at PROTEAS and will involve new concepts that have recently emerged, currently not investigated at PROTEAS, with the focus on the increase of the overall charging, discharging and storage efficiencies of the system.

Particularly, we are investigating an innovative design for an alternative receiver and tank setup that is an improvement of the initial one. Such system will be modeled and simulated to assess its characteristics and to quantitatively establish its performance improvements over the current setup present at PROTEAS. To achieve that, For that purpose we will use Computational Thermo-Fluid Dynamic Simulations in OpenFoam. Additionally energy and exergy analyses will be performed in an attempt to extract certain measures for the energy efficiency of the system.

The models used for this comparison will be experimentally validated through experiments performed at the PROTEAS Facility.

The main goals of this optimization effort are to simultaneously improve the thermodynamic efficiency of the receiver-tank system and further integrate the two components into one integrated system. The former will make the system more productive in terms of useful energy generated and the later will reducing complexity, maintenance, operational (OPEX) and capital costs (CAPEX).

Some preliminary results will be shown at in the conference.

[1] Papanicolas, C. N., A. M. Bonanos, M. C. Georgiou, E. Guillen, N. Jarraud, C. Marakkos, A. Montenon, et al. "CSP Cogeneration of Electricity and Desalinated Water at the Pentakomo Field Facility," 100008. Cape Town, South Africa, 2016.

[2] Georgiou, Marios C., Aristides M. Bonanos, Konstantinos G. Stokos, Constantinos C. Roussos, Efstathios G. Stiliaris, and Costas N. Papanicolas. "Operational Experience of Hot Air Preheating at the PROTEAS Facility," 030016. Daegu, South Korea, 2020.

[3] E. Votyakov, C. Papanicolas. "Consistent Multiphysics Simulation of a Central Tower CSP Plant as Applied to iSTORE," Abu Dhabi, United Arab Emirates, 2017.

Photocatalytic hydrogen production by natural solar radiation at pilot scale

J. G. Villachica Llamosas¹, Jakub Sowik², A. Ruiz-Aguirre¹, S. Malato¹.

(1) CIEMAT – Plataforma Solar de Almería, Ctra. De Senés s/n, 04200 Tabernas, Almería, Spain. (2) Department of Environmental Technology, Faculty of Chemistry, University of Gdansk, Gdansk, 80-308, Poland. jgvillachica@psa.es.

The use of hydrogen as feedstock, fuel and energy is gaining rapid attention. Nowadays, the main way to produce it is by electrolysis using electricity from fossil fuels. However, hydrogen produced through renewable sources results essential to support EU's commitment to reach carbon neutrality by 2050. Specifically, hydrogen production by photocatalysis is not currently competitive, with efficiencies lower than 5 % [1]. To try to make this technology a viable renewable alternative, different strategies have been adopted in this PhD Thesis.

Among the main objectives, i) the study of novel photocatalysts for solar driven hydrogen production. Firstly, the use of different photocatalysts for the photoreforming of 0.075 M of glycerol in 25 L of demineralized water [2]: 1) TiO₂ mixed with CuO or NiO; 2) gC₃N₄-urea, gC₃N₄-urea- CuO and gC₃N₄-melamine and 3) gC₃N₄-Ru and C-Ru. The best results were obtained for the first option, namely, TiO₂ mixed with the metal Cu and Ni. For these photocatalysts, different concentrations and proportion between TiO₂ and metal were tested in order to reach the maximum efficiency. With a concentration of 50 mg/L of NiO:TiO₂, in a proportion of 1:10 resulted in a conversion of solar to hydrogen (STH) of 1.44 % (Fig. 1), while the maximum STH (1.42 %) obtained with CuO:TiO₂ was using a concentration of 100 mg/L. ii) optimization of the conditions that maximize hydrogen production for each catalyst. The following step, consisted of trying to increase the efficiency of the best photocatalysts. For that, a soft calcination was applied to the catalyst mixture CuO: TiO₂, with CuO:TiO₂ (1:10) and 100 mg/L concentration. Different temperatures (200°C, 400°C), calcination times (1h, 3h, 6h) and Cu concentration (2%Cu, 7%Cu) were tested and compared. However, the results were not better. iii) optimization of the photoreactor design. Apart from the optimization of the operation, some modifications were carried out in the pilot plant, such as, modification of the volume of head space and gas carrier to contribute to the efficiency improvement. Several advantages were reached as a higher STH and a shorter delay in the H₂ quantification. Modifications offered best operating conditions to achieved a highest hydrogen production 5.7 mmol · g⁻¹ · h⁻¹. iv) Simultaneous hydrogen production, decontamination and disinfection of wastewater. Besides the hydrogen production, simultaneous decontamination and disinfection of wastewater, was also evaluated with recalcitrant organic contaminants, as imidacloprid, and a standard water pathogen *Escherichia coli*. A complete elimination of

imidacloprid and bacterium was reached after 180 min and 10 min respectively, with simultaneously hydrogen production. Finally, the study of different natural water qualities is currently being evaluated with the mixture NiO:TiO₂ (1:10) in different concentrations (50 mg/L, 100 mg/L, 200 mg/L) in order to evaluate the photocatalytic hydrogen production under realistic conditions.

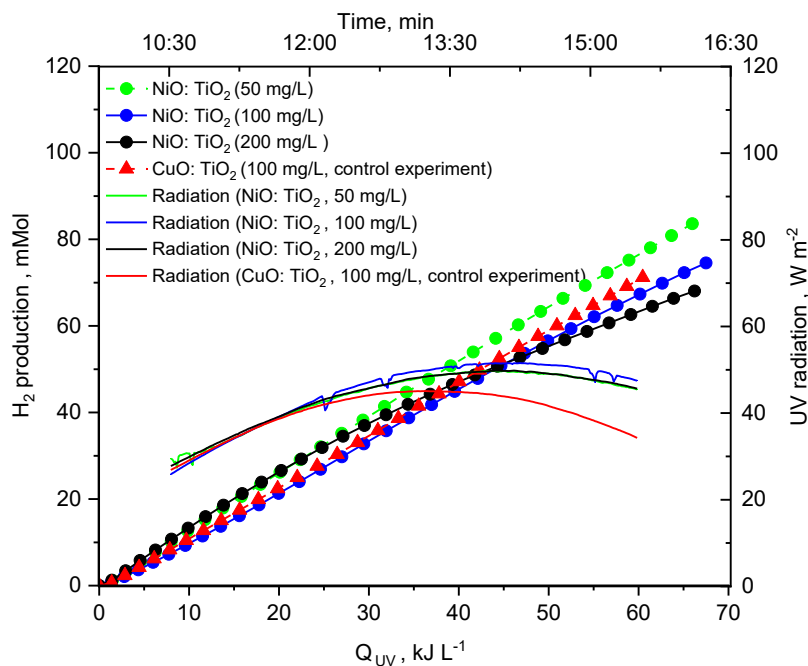


Fig. 1. Photocatalytic H₂ generation with NiO: TiO₂ (1:10) compared to control experiment with CuO:TiO₂ (1:10). Reaction conditions: glycerol 0.075 M, V = 25 L.

[1] Z. Wang, C. Li, K. Domen, Chem. Soc. Rev. 48 (2019) 2109-2125.

[2] A. Ruiz-Aguirre, J. G. Villachica-Llamas, M. I. Polo-López, A. Cabrera-Reina, G. Colón, J. Peral, S. Malato. Energy, in press.

Sweaped, Open, Moving Particle Reactor with Intrinsic Heat Recovery for Solar Thermochemical Hydrogen Production

Anika Weber, Johannes Grobbel, Christian Sattler

German Aerospace Center (DLR), Institute for Future Fuels

Anika.Weber@dlr.de

Carbon neutral production of hydrogen is one promising way to achieve the target of climate neutrality by 2050 [1]. Besides electrolysis driven by photovoltaics, one way of green hydrogen production is the implementation of a thermochemical redox cycle.

In this cycle, a redox material is first endothermically reduced under the release of oxygen at high temperatures (around 1500 °C) and low oxygen partial pressures. While high temperatures can be reached by concentrated solar radiation (CSP), low oxygen partial pressures can be reached by vacuum approaches, sweep gas or a combination of both. In a second step, the redox material is re-oxidized at significantly lower temperatures around 900 °C. Using water vapor as oxidizer, hydrogen emerges. It is also possible to use a mixture of carbon dioxide and steam as oxidizer to create synthetic gas, which can be converted to kerosene using a Fischer-Tropsch process. After oxidation, the redox material can be reused for the reduction process. [2]

This cycle has successfully been demonstrated within the Sun-to-Liquid project, achieving a record high solar-to-fuel efficiency of 5.25 % [3, 10]. In order to compete with hydrogen production via PV and electrolysis approaches, higher efficiencies are necessary. Unfortunately, existing reactor concepts, which implement thermochemical cycles, lack either demonstration or show still rather low solar-to-fuel efficiencies [4-8]. Hence, a novel high-efficiency reactor being less prone to failures shall be developed.

We present a novel moving bed particle reactor concept [9], which makes use of a simplified design. It eliminates the need for complicated and expensive high temperature moving reactor parts, high temperature vacuum or window. The concept offers the possibility for continuous production of solar fuels and is explained shortly below.

Firstly, the particles are assumed to be heated to 1450 °C in an open receiver by CSP under ambient conditions. In case of reduced power input due to, for instance, clouds, the particle flow rate can be adapted so that a high off design point flexibility is achieved. Secondly, after heating, the particles are fed into a direct contact heat exchanger (RHX), where sweep gas such as nitrogen is used as heat transfer media. The sweep gas has a dual use functionality as it not only cools down the ceria but also reduces the oxygen partial pressure so that the reduction takes place and re-oxidation is prevented. The hot sweep gas can in turn be used to preheat the particles before they enter the receiver in a second heat exchanger. The sweep gas, which is enriched with oxygen due to the reduction, is assumed to be cleaned by a ceramic membrane, which can operate at high temperatures. Thirdly, after the RHX, the particles are transported to the oxidation chamber, where the oxidation takes place at preliminary estimated pressure of 1 bar and temperature of 900 °C. The oxidation and reduction step are only weakly coupled, which is beneficial in terms of off design point flexibility.

A steady state, 0D modeling approach in Python is used to determine the energy flows and estimate the efficiency of the concept. The sweep gas demand is calculated for each aimed partial pressure according to [11]. The effect of different particle sizes ranging from micro- to milli meter range on pressure drop, temperature gradient and system efficiency is analyzed. The pressure drop is calculated following Ergun's law. The heat exchanger is assumed as cuboid with a specific width and depth, and both parameters are varied within a design study. Outlet temperatures of the heat exchangers are modeled according to the $\varepsilon - NTU$ method. The oxidation is considered in more detail following the Van 't Hoff equation and law of mass action. Spillage (radiation onto the receiver but not within the aperture) is estimated by an intercept efficiency. It is assumed that this spillage can be used either in form of heat or electricity to meet parasitic demands such as sweep gas cleaning, blowing and heating of oxidizer. The system model is completed by considering also the heliostat field efficiency. Note that any mechanical work is not considered as it is assumed to be rather negligible [12].

The model shows that the amount of sweep gas should be selected in such a way that optimum heat recovery is achieved ($\dot{C}_{\text{sweepgas}} = \dot{C}_{\text{particle}}$). At this ratio, the energy share of the chemical reaction is more than four times that of the Sun-to-Liquid reactor concept, while the sensible heat demand for the particles is reduced to less than a fifth. This result is reflected by a 'complete' efficiency from solar irradiation impinging onto the fields to the produced hydrogen (considering the higher heating value) of more than 10 %. A solar-to-fuel efficiency - according to the definition in [13] - of more than 20 % can be achieved while simultaneously avoiding technical issues.

- [1] European Commission, The European Green Deal, 2019.
- [2] C. Agrafiotis, M. Roeb, C. Sattler, in *Comprehensive Energy Systems vol. 4*, I. Dincer (Eds.), Oxford, Elsevier, 2018.
- [3] S. Zoller, E. Koepf, P. Roos, A. Steinfeld, *J. Sol. Energy Eng.*, 141 (2) (2019) 021014.
- [4] S. Siegrist, H. von Storch, M. Roeb, C. Sattler, *J. Sol. Energy Eng.*, 141 (2) (2019) 021009.
- [5] R. B. Diver, J. E. Miller, M. D. Allendorf, N. P. Siegel, R. E. Hogan, *J. Sol. Energy Eng.*, 130 (4) (2008) 041001.
- [6] I. Ermanoski, N. P. Siegel, E. B. Stechel, *J. Sol. Energy Eng.*, 135 (3) (2013) 031002.
- [7] M. Welte, R. Barhoumi, A. Zbinden, J. R. Scheffe, A. Steinfeld, *Ind. Eng. Chem. Res.*, 55 (2016) 10618 – 10625.
- [8] A. Singh, J. Lapp, J. Grobbel, S. Brendelberger, J. P. Reinhold, L. Olivera, I. Ermanoski, N. P. Siegel, A. McDaniel, M. Roeb, C. Sattler, *Solar Energy*, 157 (2017) 366-376.
- [9] A. Weber, J. Grobbel, C. Sattler, *Solar Energy*, soon to be submitted.
- [10] E. Koepf, S. Zoller, S. Luque, M. Thelen, S. Brendelberger, J. González-Aguilar, M. Romero, A. Steinfeld, *AIP Conference Proceedings SolarPACES*, Casablanca, Morocco, 2018, 2126.
- [11] S. Brendelberger, M. Roeb, M. Lange, C. Sattler, *Solar Energy*, 122 (2015) 1011-1022.
- [12] C. Falter, R. Pitz-Paal, *Solar Energy*, 176 (2018) 230-340.
- [13] B. Bulfin, M. Miranda, A. Steinfeld, *Front. Energy Res.* 9 (2021) 677980.

Reactor and system modelling for solar production of ethylene from H₂O and CO₂

David Brust, Michael Wullenkord

German Aerospace Center (DLR), Institute of Future Fuels

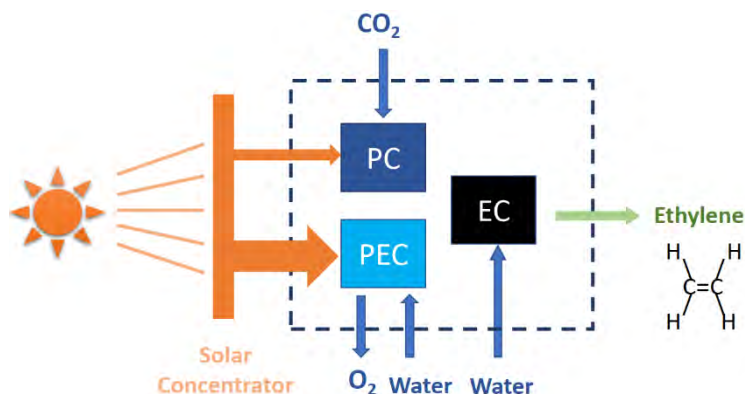


Fig. 2. Process scheme of [FlowPhotoChem](#) integrated system for ethylene production from CO₂ and water using concentrated sunlight

The production of green ethylene (C₂H₄), an important raw material in the plastics industry (e.g. polyethylene), offers a pathway towards carbon neutral feedstocks of the chemical industry, which is nowadays a large contributor to greenhouse gas emissions. Within the EU project [FlowPhotoChem](#) a system of modular flow reactors for the solar driven production of ethylene from carbon dioxide (CO₂) and water (H₂O) as shown in Fig. 1 will be developed and demonstrated experimentally.

The applied reactor technologies include a photoelectrochemical (PEC) reactor, a photocatalytic (PC) reactor and an electrocatalytic reactor (EC) which are combined together to form an integrated system. For optimal design and operation of the integrated system, semi-empirical simplified reactor models can simulate and predict the reactor performance characteristics (e.g. conversion, selectivity, efficiency) as a function of the operating conditions (e.g. temperature, pressure, species composition). The model parameters and their dependence on operating conditions can be obtained from parameter fit to experimental data.

The PEC reactor consists of a triple junction PV module for operation under concentrated sunlight (CPV) electrically connected to a proton exchange membrane water electrolyser (PEMWE) and performs the water splitting reaction to obtain hydrogen (H₂) utilising concentrated solar radiation. The PEMWE current-voltage characteristics are obtained by addition of current and temperature dependent overpotentials to the reversible cell voltage [1]. The CPV is described by a temperature dependent equivalent circuit model [2].

In the PC reactor the produced H₂ reacts with CO₂ at an immobilised heterogeneous photocatalyst under concentrated solar radiation to form carbon monoxide (CO) and H₂O

(reverse-water-gas-shift reaction, RWGS). For the mildly endothermic RWGS reaction, studies on photo-driven CO₂ hydrogenation suggest a photothermal effect [3,4], where the concentrated radiation is responsible for an increase in the irradiated catalyst surface temperature, driving the reaction. This motivates the modelling of the RWGS reaction in the photocatalytic reactor based on thermocatalyst kinetics [5] that have been studied in the literature. The simplified reactor model is derived by coupling RWGS kinetics with heat and mass transfer processes and solving the resulting partial differential equation systems using the finite volume method.

The following EC reactor reduces the carbon monoxide electrochemically to ethylene with water as the proton source. Its current-voltage characteristic is obtained by combining experimentally obtained half-cell potentials with the cell ohmic overpotential from EIS measurements [6,7]. The faradaic efficiency towards the CO reduction products at the cathode is described by Tafel kinetics for each observed product where kinetic parameters for each product are fitted separately.

Introducing these simplified reactor models into a flowsheet together with piping and balance-of-plant components, a process simulation is obtained. This allows the simulation of an integrated system with respect to mass, chemical species and energy balances. Furthermore, questions of reactor sizing (scale-up or numbering-up), selection and sizing of balance-of-plant components, and heat integration potential are addressed with subsequent optimisation of operating conditions to maximise solar-to-chemical conversion efficiency at the system level.

- [1] Suermann, M., T. J. Schmidt and F. N. Büchi, *Electrochimica Acta* 211 (2016) 989-997.
- [2] Segev, G., G. Mittelman and A. Kribus, *Solar Energy Materials and Solar Cells* 98 (2012) 57-65.
- [3] Jia, J., P. G. O'Brien, L. He, Q. Qiao, T. Fei, L. M. Reyes, T. E. Burrow, Y. Dong, K. Liao, M. Varela, S. J. Pennycook, M. Hmadeh, A. S. Helmy, N. P. Kherani, D. D. Perovic and G. A. Ozin, *Adv Sci (Weinh)* 3(10) (2016).
- [4] Xu, Y. F., P. N. Duchesne, L. Wang, A. Tavasoli, A. A. Jelle, M. Xia, J. F. Liao, D. B. Kuang and G. A. Ozin, *Nat Commun* 11(1) (2020).
- [5] Ginés, M. J. L., A. J. Marchi and C. R. Apesteguía, *Applied Catalysis A: General* 154(1-2) (1997) 155-171.
- [6] Romero Cuellar, N. S., C. Scherer, B. Kaçkar, W. Eisenreich, C. Huber, K. Wiesner-Fleischer, M. Fleischer and O. Hinrichsen, *Journal of CO2 Utilization* 36 (2020) 263-275.
- [7] Endrodi, B., A. Samu, E. Kecsenovity, T. Halmagyi, D. Sebok and C. Janaky, *Nat Energy* 6(4) (2021) 439-448.

The project FlowPhotoChem has received funding from the European Union's Horizon 2020 research and innovation programme under grant agreement No 862453.

Get the right feature:

Tailoring of material properties by Sr content in $\text{Ca}_{1-x}\text{Sr}_x\text{MnO}_{3-\delta}$

Lena Klaas^{1,*}, Brendan Bulfin², Alexander Francke³, Dorottya Kriechbaumer¹, Martin Roeb¹, Christian Sattler¹

¹ Deutsches Zentrum für Luft- und Raumfahrt - DLR / German Aerospace Center, Institute of Future Fuels, Linder Höhe, 51147 Cologne, Germany; ² ETH Zürich, Department of Mechanical and Process Engineering, 8092 Zürich, Switzerland; ³ Deutsches Zentrum für Luft- und Raumfahrt - DLR / German Aerospace Center, Institute of Materials Research, Linder Höhe, 51147 Cologne, Germany
*Lena.Klaas@DLR.de

$\text{CaMnO}_{3-\delta}$ based perovskites are applied in several thermochemical processes like oxygen partial pressure adjustment, looping processes and thermochemical heat storages. Here, their applicability is determined primarily by structural stability, thermodynamic properties and redox kinetics.

To enable the tailoring of these important properties, we investigate the effects of Sr content in $\text{Ca}_{1-x}\text{Sr}_x\text{MnO}_{3-\delta}$.

In Fig. 4 the ideal cubic perovskite structure is displayed and the different atoms labelled. Due to the ionic radii, $\text{Ca}_{1-x}\text{Sr}_x\text{MnO}_{3-\delta}$ has an orthorhombic distortion. We show the effect of the Sr content ($x \in [0, 0.4]$) on the structure and distortion by X-ray powder diffraction measurements (XRD). Using in situ high-temperature XRD at temperatures up to 1373 K and with 1 % and 20 % O_2 in the atmosphere, we investigate the expansion and phase change of the material ($x \in [0, 0.2]$). The impact of the Sr content on the thermodynamic properties is analysed by thermogravimetric measurements (TGA), using the van't Hoff approach. The activation energy of the oxidation is extracted from TGA measurements by varying the oxidation temperature and oxygen partial pressure. Moreover, it is shown that the diameter of granules between 1.25 mm and 2.44 mm does not impact the oxidation kinetics.

Concluding with a discussion how the trends observed in the structural analysis might explain the observed thermodynamic properties.

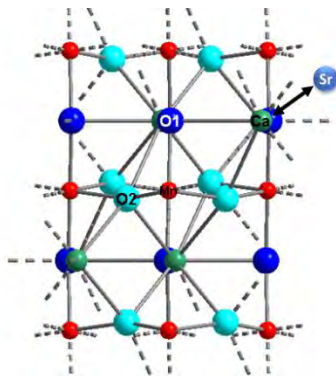


Fig. 4 – Ideal cubic perovskite structure of $\text{Ca}_{1-x}\text{Sr}_x\text{MnO}_{3-\delta}$

Computational screening and experimental validation of binary and ternary metal nitrides for the solar-driven thermochemical production of green ammonia

Daniel Notter¹, María-Elena Gálvez², Brendan Bulfin¹, Aldo Steinfeld¹.

¹ *Department of Mechanical and Process Engineering, ETH Zurich, 8092 Zurich, Switzerland. danotter@ethz.ch*

² *Sorbonne Université, CNRS, UMR 7190, Institut Jean le Rond d'Alembert, F-75005 Paris, France.*

The current conventional production of ammonia relies on the well-known Haber-Bosch process, involving a catalytic high-pressure reaction between H₂ and N₂. Due to the production of H₂ and N₂ based on highly energy-intensive processes using fossil fuels, the worldwide ammonia production is responsible for 1.2% of the anthropogenic global greenhouse gas emissions. Furthermore, the high pressures needed to increase the yield and the large recycle flows of the unreacted H₂ and N₂ impose demanding requirements on the equipment, increasing the cost and complexity of the process and favouring large, centralized plants. Multi-step thermochemical cycles based on metal nitrides stand as a promising alternative to this process, since they can substantially mitigate or even eliminate the concomitant CO₂ emissions linked to ammonia production. In such cycles, concentrated solar energy is used to supply the high-temperature heat required in the endothermic reaction steps. Previous studies have proven successful synthesis of ammonia at much lower pressures – even around ambient conditions. Nevertheless, the availability of literature and experimental data on the metal nitrides involved in these cycles is scarce. In an effort to investigate a broader range of candidates, this work presents the results of a screening of different metal nitride compounds using DFT (Density Function Theory) calculations from open-access databases. The probable reaction pathways encompassing either the hydrogenation (H₂) or the hydrolysis (H₂O) of such nitrides, as well as their re-nitridation to recycle the pristine metal nitride were identified through a Gibbs free energy minimization algorithm. The experimental validation of the selected candidates was conducted both through dynamic thermogravimetric analysis (TGA) and in a high-pressure reactor. Finally, the different fresh and spent materials were submitted to physicochemical characterization, to evaluate the chemical, structural and morphological changes inferred through hydrogenation/hydrolysis/re-nitridation and aiming to assess their performance under cyclic operation.

Dry Redox Reforming

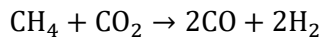
Mario Zuber¹, Simon Ackermann², Aldo Steinfeld¹

¹*Professorship of Renewable Energy Carriers, ETH Zurich, Switzerland*

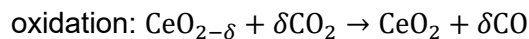
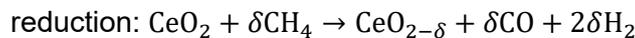
mazuber@ethz.ch

²*Synhelion SA, Switzerland*

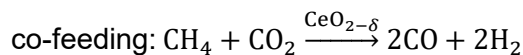
Thermochemical processes driven by concentrated solar energy offer an efficient pathway to the production of sustainable fuels. A precursor to such liquid fuels is syngas, a mixture of H₂ and CO. A means of producing syngas is via dry reforming of CH₄, whereby, the sensible and reaction heat is supplied by concentrated solar energy:



Within this context CeO₂ is introduced as an active redox reactor material over which the dry reforming reaction can occur. This avoids the use of additional catalyst, unwanted side reactions, and serves as a bridge technology to the solar-driven production of syngas from H₂O and CO₂ via a ceria-based redox cycle. The dry redox reforming cycle process is represented by:



δ represents the non-stoichiometry of CeO₂. The process operates isobarically and isothermally in the range of 800-1200°C. The dry redox reforming process can also be performed by co-feeding CH₄ and CO₂:



We report on further developments in characterization of the dry redox reforming system on the theoretical, experimental, and computational fronts. A tubular reactor ($\varnothing=19$ mm, $l=200$ mm) is used as a validation tool for the computational fluid dynamic model made using OpenFOAM.

Fully-automated Solar Fuel System for the Thermochemical Production of Syngas from H₂O and CO₂ applicable for Methanol or Fischer-Tropsch Synthesis

Remo Schächli¹, Aldo Steinfeld¹

¹ *Department of Mechanical and Process Engineering, ETH Zürich, 8092 Zürich, Switzerland
schremo@ethz.ch*

We report on the design and operation of a modular and fully-automated solar fuel system for the solar thermochemical production of syngas – a specific mixture of CO and H₂ – from CO₂ and H₂O via a ceria-based redox cycle using concentrated solar energy.

The solar reactor for effecting this redox cycle consists of a cavity-receiver containing a reticulated porous ceramic (RPC) foam structure made of pure CeO₂. Two identical solar reactors are mounted side-by-side on the focus of a solar dish concentrator that enables the operation of both solar reactors simultaneously by alternating the solar radiative input between them. Thus, while one solar reactor is performing the endothermic reduction step on sun at 1500 °C and 40 mbar, the second solar reactor is performing the exothermic oxidation step off sun at below 900 °C and 1 bar.

The syngas composition can be tailored by changing H₂O:CO₂ feed ratios as well as choosing adequate oxidation start/end conditions to meet the desired quality and stoichiometry suitable for Fischer-Tropsch or methanol synthesis. Thus, the need for additional downstream refining of the syngas, e.g. via the energy-intensive reverse water-gas shift reaction, is eliminated.

The entire system is controlled to perform fully automated consecutive redox cycles. Further, the operation parameters, namely reduction/oxidation temperatures, gas flow rates, or oxidation start/end conditions, are continuously updated based on real-time product gas analysis and feedback loops. We present representative on-sun runs with fully-automated consecutive redox cycles and show the operational parameter analysis aimed at optimising syngas quality, fuel yield, energy efficiency and mass conversion.

Solar calcination of non-metallic minerals: metakaoline production to synthesize zeolites

Pelin Paşabeyoğlu^{1,2}, Gkiokchan Moumin³, Burcu Akata^{1,2}

1. Middle East Technical University (METU), Department of Micro and Nanotechnology, Ankara, Turkey, paltay@metu.edu.tr

2. Central Laboratory, Middle East Technical University (METU), Ankara, Turkey

3. Department of Solar Chemical Engineering, DLR, Cologne, Germany

Several minerals require a thermal treatment prior to their application as mineral feedstock and use in the production of value-added products. Calcination of minerals is mostly done by burning fossil fuels and takes place at temperatures ranging from 500 to 1300 °C [1]. These thermal processes are energy-consuming, partly due to the preheating of the minerals to their reaction temperature. Renewable energies such as Concentrated Solar Thermal (CST) can be a good candidate for industrial processes such as calcination, that conventionally require fossil fuels to generate electricity.

The zeolite industry has become more and more competitive over the years such that finding the best, the fastest but the lowest production cost synthesis route is a priority. Traditionally, zeolites are synthesized by hydrothermal crystallization of specially prepared silicon, aluminum, and sodium solution. Replacing conventional chemicals with low-cost raw materials such as minerals has been gaining attention in countries where natural sources are exported with no added value. Creating an industrial use in which raw materials are transformed into valuable products is desired. Since fusion/calcination step in the synthesis of zeolites from natural sources is the most energy-consuming and expensive step; alternative methods to prepare meta forms of natural sources have been investigated [2]–[4]. One promising route for the fusion/calcination step is CST energy, in particular with point focus technology such as solar towers. Since Turkey has a very promising combination of abundant feedstock for zeolites and solar resources, this can be seen as a preliminary step towards realizing such applications.

This research focuses on solar calcination of aluminosilicate mineral kaolinite to produce meta form that is eligible as precursor for zeolite synthesis. Kaolinite is loaded in a rotary kiln and solar simulator is used for calcination at temperatures 650-1000°C for at least two hours. Temperatures are measured by thermocouples located inside and outside of the kiln. After the calcination process, solar-produced meta forms of the kaolinite are used to synthesize zeolite 4A and zeolite 13X by a simple method. Results show that solar calcined raw materials are as good and efficient as the conventionally calcined raw materials in terms of supplying the meta forms for the zeolite synthesis. The overall results suggest that solar calcination is a good alternative to mass produce meta forms of the minerals to use in the synthesis of value-added products such as zeolites.

Acknowledgements

The author wishes to thank SolarTwins project funded by European Union Horizon 2020 under grant agreement SOLARTWINS-GA No:856619.



References

- [1] E. Benhelal, G. Zahedi, E. Shamsaei, A. Bahadori, *Journal of Cleaner Production*, 51 (2013) 142-161
- [2] J. Baeyens, H. Zhang, W. Kong, P. Dumont, and G. Flamant, *AIP Conf. Proc.*, Casablanca, Morocco, 2019, 2126, 180002
- [3] T. Esence, E. Guillot, M. Tessonneaud, J. L. Sans, and G. Flamant, *Solar Energy*, 207 (2020), 367–378
- [4] S. K. Kirdeciler and B. Akata, *Adv. Powder Technol.*, 31 (2020), 4336–4343

Experimental Assessment of Solar Methane Pyrolysis in a Molten-Tin Bubble Column Reactor

Malek MSHEIK, Sylvain RODAT, Stéphane ABANADES

Processes, Materials and Solar Energy Laboratory, PROMES-CNRS, 7 Rue du Four Solaire, 66120 Font Romeu, France. E-mail: malek.msheik@promes.cnrs.fr

1. Introduction

Solar methane pyrolysis allows hydrogen production with zero-CO₂ emissions. The pyrolysis reaction results in hydrogen and solid carbon. Methane was so far mostly decomposed in gaseous media, whether catalyzed (using either metallic or carbonaceous catalysts) or not. In such a path, the catalyst may ultimately deactivate by coking, and the reactor can be clogged due to carbon sticking on the hot reactor walls. Solar methane pyrolysis in molten tin was investigated and compared to gas-phase reaction. By bubbling methane in liquid tin, heat transfer should be improved since liquids are better heat conductors than gases. Moreover, carbon separation may be easier since carbon floats atop the liquid bath due to density difference with tin, therefore clogging should be avoided [1]. Methane pyrolysis in melts is a new approach and has never been investigated in solar reactors yet.

2. Methodology

Experiments were conducted using a tubular solar reactor designed and installed at PROMES-CNRS in Odeillo, France. The reactor consists of two concentric alumina tubes (outer tube, closed at one end: L=315 mm, D_i=23 mm, D_{out}=30 mm; inner tube: L=500 mm, D_i=3 mm, D_{out}=6 mm), surrounded by insulation layers to limit heat losses and thermocouples to measure the temperature. Two different configurations were compared: methane pyrolysis in gas phase (uncatalyzed) and in molten tin with bath height = 120 mm. Methane, diluted with argon, was flowed or bubbled in the reactor where it decomposed under solar heating through a 1.5 kW solar furnace concentrating system. Effects of parameters like temperature (T) (1000-1400°C), inlet gas flow rate (Q₀) (0.5-1 NL/min), inlet methane mole fraction (y_{0,CH₄}) (0.1-0.3-0.5) were studied separately by fixing other parameters' values and only changing the parameter of interest. Effects of Q₀ and y_{0,CH₄} will be detailed later.

3. Results and discussion

When T was increased (1000-1400°C) with y_{0,CH₄}=0.3 and Q₀=0.5 NL/min, methane conversion rose in both routes (gas phase: 2-98%, molten tin: 0-91%) (Fig.1. (a)). This result was expected because pyrolysis is an endothermic reaction and according to Le Chatelier's principle, increasing the temperature shifts the reaction to the right (more products: H₂ and C).

Regarding the effect of the medium type on methane pyrolysis, the decomposition extent in molten tin was lower than in gas phase at all temperatures (Fig.1. (a)). To understand this result, bubbles' diameter (D_b) was estimated using Tate's law [2] and found equal to 5.2 mm. Such a relatively large diameter resulted in lower bubbles' rising time (space-time) than gas space-time in gas phase (0.5 s vs. 0.83 s at $Q_0=0.5$ NL/min) (Fig.1. (b)). Moreover, such large bubbles led to small gas-tin surface contact, limiting the heat transfer between hot liquid tin and gas. The collected carbon product was analyzed and found to be carbon black in gas phase (particle size: 50-100 nm), while it was sheet-like in molten tin. Energy dispersive X-Ray analysis was performed to determine carbon tin contamination levels.

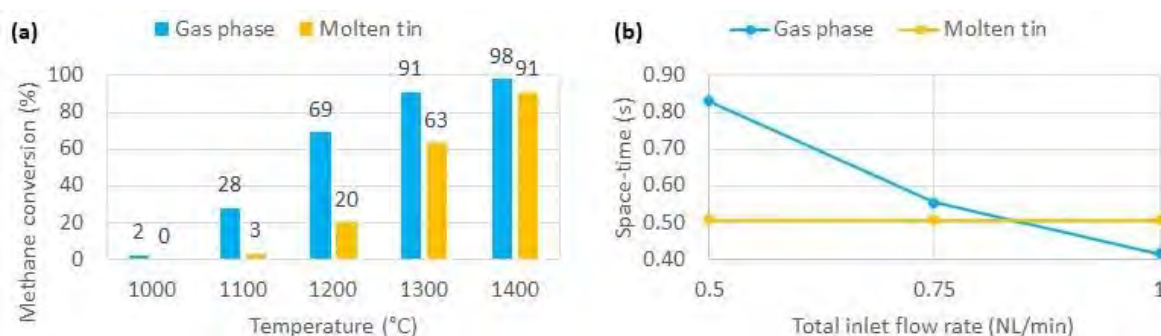


Fig.5. (a) Methane conversion as a function of temperature ($Q_0=0.5$ NL/min, $y_{0,CH_4}=0.3$) (b) Space-time as a function of gas inlet flow rate ($T=1300^\circ\text{C}$, $y_{0,CH_4}=0.3$).

4. Conclusion

Methane pyrolysis in molten tin was compared to uncatalyzed pyrolysis in gas phase in a dedicated solar reactor. Increasing temperature boosted methane conversion (endothermic reaction). Methane conversion was higher in gas-phase pyrolysis due to longer gas residence time as compared to molten-tin pyrolysis. Generating smaller bubbles through smaller feeder diameter or by the set-up of gas spargers could boost conversion thanks to better heat and mass transfer (larger gas-liquid interface) and longer bubble residence time. The use of catalytic molten media is also a perspective for future investigations on bubbling solar reactors.

[1] Msheik M, Rodat S, Abanades S, Methane Cracking for Hydrogen Production: A Review of Catalytic and Molten Media Pyrolysis, *Energies* 2021; 14:3107. <https://doi.org/10.3390/en14113107>.

[2] Paxman D, Trottier S, Nikoo M, Secanell M, Ordorica-Garcia G, Initial Experimental and Theoretical Investigation of Solar Molten Media Methane Cracking for Hydrogen Production, *Energy Procedia* 2014; 49:2027–36. <https://doi.org/10.1016/j.egypro.2014.03.215>.

Modelling and Performance Analysis of a SOE System integrating PV, Concentrating Solar Heat and Thermal Energy Storage

B. Herrero Badorrey^{1*}, J. González-Aguilar¹ and M. Romero¹

¹High Temperature Processes Unit, IMDEA Energy, Avda. Ramón de la Sagra 3,
28935 Móstoles, Spain

(*) beatriz.herrero@imdea.org

This work describes the flow sheeting, modelling and performance analysis of a high temperature electrolysis system, consisting of a Solid Oxide Electrolysis Cell (SOEC) coupled with a PV plant, a Solar Collector Assembly (SCA) of parabolic troughs and a Thermal Energy Storage (TES) system, developed within the EU-FCJU PROMETEO project. This new concept reduces the electricity demand of the electrolysis process and ensures flexible hydrogen production thanks to the TES. It aims to use intermittent renewable energies to feed the SOEC (concentrating solar for the thermal input and PV for the electric input). Decoupling hydrogen production from heat availability is key for several end-user applications i.e. grid services, curtailment or chemical industry, as it makes feasible to produce hydrogen on-demand or whenever renewable electricity is available. A small system (25kWe SOEC) has been modeled using the software EcosimPro for future optimization of component sizing and operational strategies. The main components of the prototype are the SCA, the TES and the SOEC. A model for each of them has been developed and validated. Apart from these models, other components required for the Balance of Plant (BoP) of the system, such as heat exchangers, evaporators, electric heaters, etc. have been created.

Solar collector Assembly (SCA) and TES

A solar collector assembly model has been developed using EcosimPro. The model is based on the one used by System Advisor Model (SAM), <https://sam.nrel.gov/>, and the results of the simulation have been validated with the ones obtained using SAM. The commercial parabolic trough model Luz LS-2, the Schott PTR70 receiver tube, and Therminol VP-1 as Heat Transfer Fluid (HTF) have been chosen. Apart from providing hourly data of thermal energy generation, the SCA model calculates the required number of rows and collectors per row in order to achieve the desired thermal power output in the design point. A Typical Meteorological Year (TMY) file is required as an input to perform all the calculations. The analysis is done for the city of Cuenca, Spain. The low temperatures present in this system do not allow using conventional CSP thermal storage systems. Thermal energy is used to evaporate the water before it enters the electrolyser, steam is required at ~133 °C and common used Molten Salts (MS) fusion temperature occurs at ~280 °C. A two-tanks storage system filled with MS (HITEX XL) has been modeled and validated. Whenever thermal power is available (~10 AM – 19 PM) steam is directly generated with the hot HTF coming from the SCA. The remaining hot HTF mass flow (generated but not used to evaporate) is directed to a HEX in order to heat up cold MS and store them in the hot MS tank. When there is no thermal power coming from the solar field, or it is not enough to produce steam, hot MS are directed to a second HEX to heat up HTF, use it to evaporate and then store the cooled MS in the cold tank.

Solid Oxide Electrolysis Cell (SOEC)

Table 1. SOEC inlet and outlet values

SOEC Energy and Mass Balance	Unit	Value
Voltage full power (Thermoneutral)	V	1.32
Current at full power	A	235
Steam Utilization	%	70
Hydrogen inlet ratio (cathode)	% v/v	10
Hydrogen production	kg/h	0.82
Anode airflow (dry air)	kg/h	26.7
Cell temperature	K	1066

The SOEC model, based on the ones proposed by [1] and [2], consists in two iterative loops, the first one calculates the mass balance in the electrolysis cell and the second one the energy balance. By imposing the initial gas composition and cell temperature, the cell current density, voltage and temperature and the mass flow rates of hydrogen and oxygen leaving the cell are calculated. Moreover, it allows to select different operating modes. On the system level, the electrolyser can work either with constant steam-H₂ conversion (inlet flow rate is a function of the inlet power load) or constant inlet flow rate (steam conversion is a function of the inlet power load). On the cell level, two modes are possible: inlet temperature varies to maintain the thermoneutral condition; or inlet temperature is kept constant, this will lead to a situation where the cell would pass through endothermal, thermoneutral and exothermal modes along the inlet power range. The component has been developed in EcosimPro and validated with the results from [1]. Table 1 shows the energy and mass balance results obtained in the design point and the inlet parameters for the PROMETEO prototype: 25kW SOEC with 80 cells of 320 cm².

Performance Analysis

Apart from simulations at design point, the thermal input solar share of the system has been analyzed. Thus, a performance analysis was carried out for a complete year using EcosimPro. The simulation case is 24/7 hydrogen production with PROMETEO stack at full power (25 kW), constant steam conversion (70%) and thermoneutral condition connected to a 15kW solar thermal field with 16h TES.

The solar field outlet power distribution and the power source used to evaporate have been studied for every hour of a year. Figure 1 shows these results for April 25th. In the left figure the distribution of the thermal power leaving the solar field can be seen: evaporator (blue), thermal storage (red) and recirculation or lost (black and white lines), this happens when the storage is already charged. The right figure shows the power source used to produce steam: solar field (yellow), thermal storage (blue) or electric heater (black and white lines).

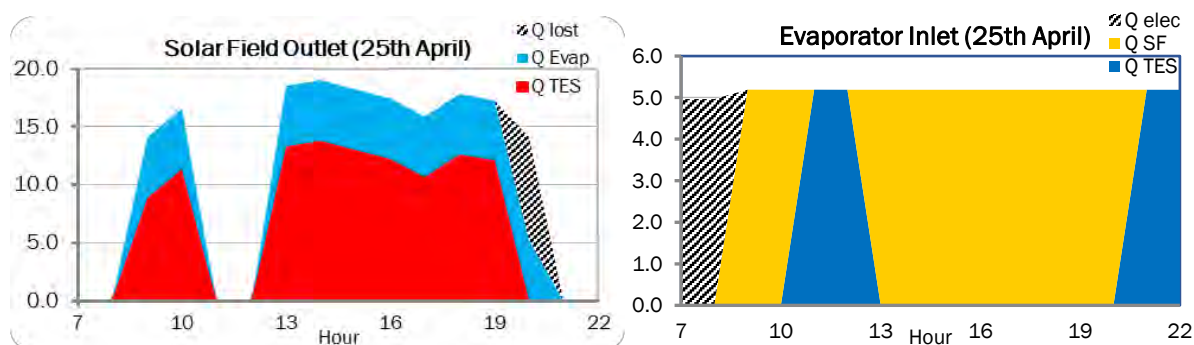


Figure 1. (Left) Solar collector outlet power distribution and (right) power sources of the evaporator.

References

- [1] Sanz-Bermejo J, Gallardo-Natividad V, Romero, M., González-Aguilar, J. Coupling of a Solid-oxide Cell Unit and a Linear Fresnel Reflector Field for Grid Management. *Energy Procedia* 2014; 57:706-15.
- [2] Floriane Petipas, Annabelle Brisse and Chakib Bouallou. Model-based behaviour of a high temperature electrolyser system operated at various loads. *Journal of Power Sources* 2013, 239: 584-595.

Natural based solutions combined with solar advanced oxidation processes for wastewater recovery

A. Hernández-Zanoletty, I. Oller, M.I. Polo-López, S. Malato.

Plataforma Solar de Almería-CIEMAT, Carretera de Senés Km 4, 04200 (Tabernas, Almería), Spain. ahernandez@psa.es

The Mediterranean Region is characterized by great water stress and scarcity due to climate change and the high water consumption in the agricultural sector. Therefore, the treatment and reuse of urban wastewater must be considered as a suitable alternative to mitigate these problems. The main problems in the recovery of wastewater is the presence of contaminants of emerging concern (CECs), pathogenic microorganisms, antibiotic resistance bacteria and genes (ARB and ARGs) or disinfection by-products. Therefore, it is necessary to implement new integrated wastewater technologies that allow improving the quality of water for reusing purposes [1].

The aim of this work is to investigate the integration of two simple, profitable and low-cost technologies at demonstrative scale including natural based solutions [2] (two wetlands, vertical and horizontal) connected with an advanced solar treatment (raceway pond reactor (RPR)) (Fig.1) for compiling with the new EU regulation on minimum requirements for water reuse, where turbidity ≤ 5 NTU and *E. coli* ≤ 10 CFU/100 mL. Nevertheless, CECs, ARB and ARGs have not been yet included.



Fig.1. Demonstration system of natural based solutions coupled with advanced solar tertiary treatment in Murcia, Spain.

Firstly, target actual urban wastewater coming from the outlet of the horizontal wetland was characterized: Dissolved organic carbon (DOC): 14.5 mg/L; $[\text{HCO}_3^-]$: 476.4 mg/L; Turbidity (NTU): 2.21; pH: 7.49; Conductivity: 4.1 mS/cm; Cl⁻: 730.4 mg/L; NO₃⁻: 4.3 mg/L; NO₂⁻: 39.5 mg/L; PO₄³⁻: 9.0 mg/L; SO₄²⁻: 892.0 mg/L; Na⁺: 468.0 mg/L; NH₄⁺: 15.2 mg/L; K⁺: 20.4 mg/L; Ca²⁺: 287.4 mg/L; Mg²⁺: 122.9 mg/L. 3-4 LRV (Logarithm Reduction Value) of *E. coli* was achieved along the wetlands, reaching the DL of 2 CFU/mL. CECs adsorption/degradation was also evaluated by LC/MS-MS, obtaining 88% of average adsorption at ng/L concentration level.

Then, the wetland effluent was preliminary treated by solar processes at lab-scale, using a 200 mL UV-transparent beaker magnetically agitated at 200 rpm under natural solar radiation and in combination with two different oxidants: H₂O₂ (at 50 and 100 mg/L) and persulfate (PS) (at 0.5 and 1 mM).

The mere effect of solar irradiance on the wetlands' outlet produced a small contaminant removal percentage (19%), in comparison with the best CEC removal obtained with the addition of 50 mg/L of H₂O₂ (47% removal). On the contrary, the addition of PS had no significant effect.

Disinfection studies were also carried out (Fig. 2) showing that the effect of PS is similar to the mere effect of only solar irradiance in both natural occurring microorganisms monitored in the wetland effluent (Total coliforms and *Salmonella spp.*), but an important inactivation was observed in the presence of the two tested H₂O₂ concentrations.

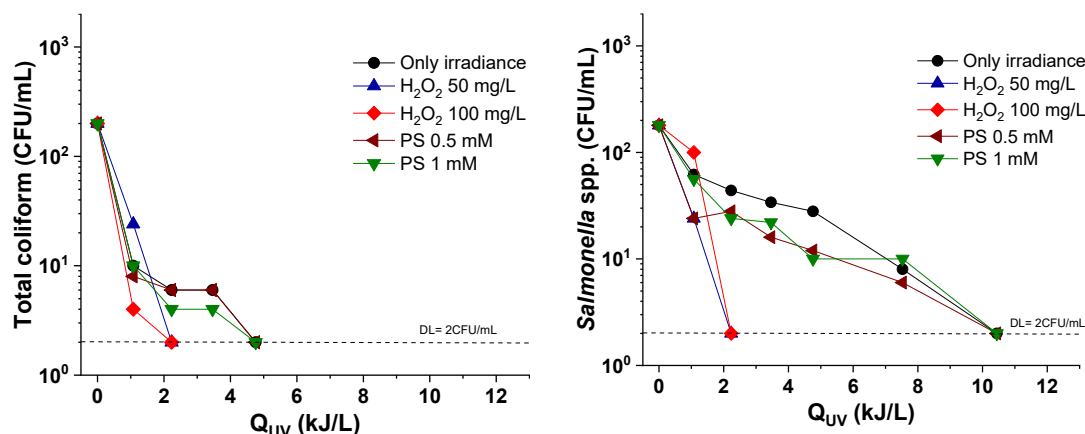


Fig.2. Inactivation profiles of Total coliform and *Salmonella spp.* in presence of different oxidant concentrations under natural solar radiation.

[1] A. Christou, A. Agüera, J.M. Bayona, E. Cytryn, V. Fotopoulos, D. Lambropoulou, C.M. Manaia, C. Michael, M. Revitt, P. Schröder, D. Fatta-Kassinos, *Water Res.* 123 (2017) 448-467.

[2] A. Haghshenas-Adarmanabadi, M. Heidarpour, S. Tarkesh-Esfahani, *Water Air Soil Pollut* (2016) 227: 28.

Acknowledgment: The AQUACYCLE project is funded and supported by the European Union through the ENI CBC Mediterranean Sea Basin Programme.

Performance comparison of commercial membrane distillation modules operating in vacuum-assisted air gap configuration for brine concentration.

I. Requena, J.A. Andrés-Mañas, G. Zaragoza

CIEMAT-Plataforma Solar de Almería, Ctra. de Senés s/n, 04200 Tabernas, Almería, Spain.

Universidad de Almería-CIESOL, Ctra. Sacramento s/n, 04120 La Cañada, Almería, Spain.

Corresponding author, email: isabel.requena@psa.es

Nowadays, seawater desalination is necessary to increase the availability of fresh water, being reverse osmosis (RO) the most widely used technology for this purpose at a large scale. This process generates a residue with salt concentration of up to 70 g/L, which dumped back into the sea in coastal areas, could cause damage to the marine ecosystem and, buried in the subsoil of inland areas, could contaminate soils and aquifers. Therefore, this residue must be properly managed. From this residue, more fresh water can be produced, as well as salts and other valuable compounds that are dissolved in seawater or groundwater. To achieve this objective, solar membrane distillation (MD) is proposed as a mean for concentrating the brine residue from current RO processes, in order to achieve zero liquid discharge (ZLD) desalination.

MD is a thermal separation process, in which only steam molecules pass through a microporous hydrophobic membrane. The driving force of MD is the vapour pressure difference between both sides of the membrane, derived from the temperature difference between them. The required temperature, in the order of 80-90 °C, can be obtained from a static solar collectors field [1]. Since the influence of salinity in vapour pressure is lesser than in the osmotic pressure, MD is more suitable than RO for treating highly concentrated solutions. Other advantages of MD are: theoretical rejection of 100% of salt, low operating temperatures and pressures, and avoidance of intensive pretreatments.

The best performance so far in pilot-scale MD has been achieved with multi-envelope spiral-wound air gap (AGMD) modules working with light vacuum (V-AGMD), which allows to suck out air from the gap [2] without altering the liquid-vapour equilibrium. This decreases the mass transfer resistance and thus enhances the vapour flux through the membrane pores [3]. However, the main disadvantage of these modules is their low recovery ratio, which is the quotient of the permeate flow rate and the feed flow rate. This increases when operating in batch, namely, recirculating the feed through the module: the brine is concentrated further and its volume reduced, as the permeate is separated.

Two multi-envelope spiral-wound modules (named AS24 and AS26) differing in the membrane area, and in the number and length of their channels, have been assessed in a thorough experimental campaign carried out at Plataforma Solar de Almería (in SE Spain). Brines between 35 to 245 g/L were used as feed. Operation was carried out at different evaporation and cooling channels inlet temperatures (60-80 °C and 20-30 °C, respectively), and feed flow rates between 400 and 1100 L/h. The system is connected to a solar thermal field of 10 flat-plate collectors with total effective area of 20 m² and able to supplying a nominal thermal power of 7 kW_{th} at an outlet temperature of 90 °C.

The internal configuration determines the residence time and the feed velocity inside the modules, which have a direct influence on their performance. This is quantified using the permeate flux and the specific thermal energy consumption (STEC). Feed residence times in modules AS24 and AS26 are similar, but feed velocity in the former is double because it has half internal channels than the latter. In addition, the feed velocity is directly proportional to hydraulic pressure drop (PDrop), and there is a limit in it to ensure that the internal structure of the module is not damaged. This limit is reached in module AS24 when operating at high feed flow rates and high salinities. For this reason, batch experiments have been carried out with the module AS26. Apart from that, AS26 is the most thermally efficient, achieving a minimum STEC of 40 kWh_{th}/m³ compared to 48 kWh_{th}/m³ of AS24 module [3].

Steady-state experiments carried out at the lowest salinities, between 35 and 105 g/L, showed that as the evaporation channels inlet temperature increases, permeate flux and thermal efficiency increase; as the feed flow rate increases, so does the production, but thermal efficiency decreases; finally, the cooling channels inlet temperature is the less influential parameter, but when it decreases, the permeate flux increases. However, for salinity of 105 g/L and above, the optimum feed flow rate increases when the salinity increases, and the cooling channels inlet temperature has more influence on the results. In batch experiments, as salinity increases, permeate flux and thermal efficiency decrease. An operational optimization will be thus necessary to control the feed flow rate and maximize the heat recovery throughout the process. This is important because the higher the thermal efficiency, the lower the consumption of the solar field will be, so there will be more thermal energy available.

[1] G. Gopi, G. Arthanareeswaran, A.F. Ismail, *Chemical Engineering Research and Design* 144 (219) 520-537.

[2] J.A. Andrés-Mañas, A. Ruiz-Aguirre, F.G. Ación, G. Zaragoza, *Desalination*, 475 (2020) 114202.

[3] J.A. Andrés-Mañas, I. Requena, G. Zaragoza, *Desalination*, 528 (2022) 115490.

Modelling and automation of a multi-effect distillation plant for the optimal coupling with solar energy

Juan Miguel Serrano, Lidia Roca, Patricia Palenzuela

CIEMAT-Plataforma Solar de Almería-CIESOL, Ctra. de Senés km 4.5, 04200 Tabernas, Spain, jmserrano@psa.es

One of the most important goals of current desalination/brine concentration technologies [1,2] is to move away from fossil fuels [3]. For Multi-Effect Distillation (MED) this means the coupling with solar thermal energy, either in a standalone water generation or in a electricity-water co-generation scheme [4]. Another option is making use of waste heat from industrial processes or alternative energy sources such as geothermal [5].

MED plants have traditionally been operated at its design conditions, for which they reach the most quantity of distillate volume per unit of energy consumed, but this mode of operation does not take into account neither the energy variability associated with renewable sources such as solar nor the availability and capacity of thermal storage. This can lead to the waste of an important fraction of the available energy. To allow for the optimal coupling of MED plants and solar energy, that is, to maximize water production over a period of time, a hierarchical control architecture is proposed [6]. It consists in two main layers, an upper layer with a longer sample period (hours), where an optimizer will make use of a model of both a solar field and an MED plant, and generate optimal operation points for both. Another layer, with a shorter sample period, that follows those reference operating points by controlling the manipulable variables from the two systems (solar field and MED plant).

Before implementing the proposed control scheme, it is required to develop its bases: modelling of the systems and automation of its operation. In this regard, two works are presented:

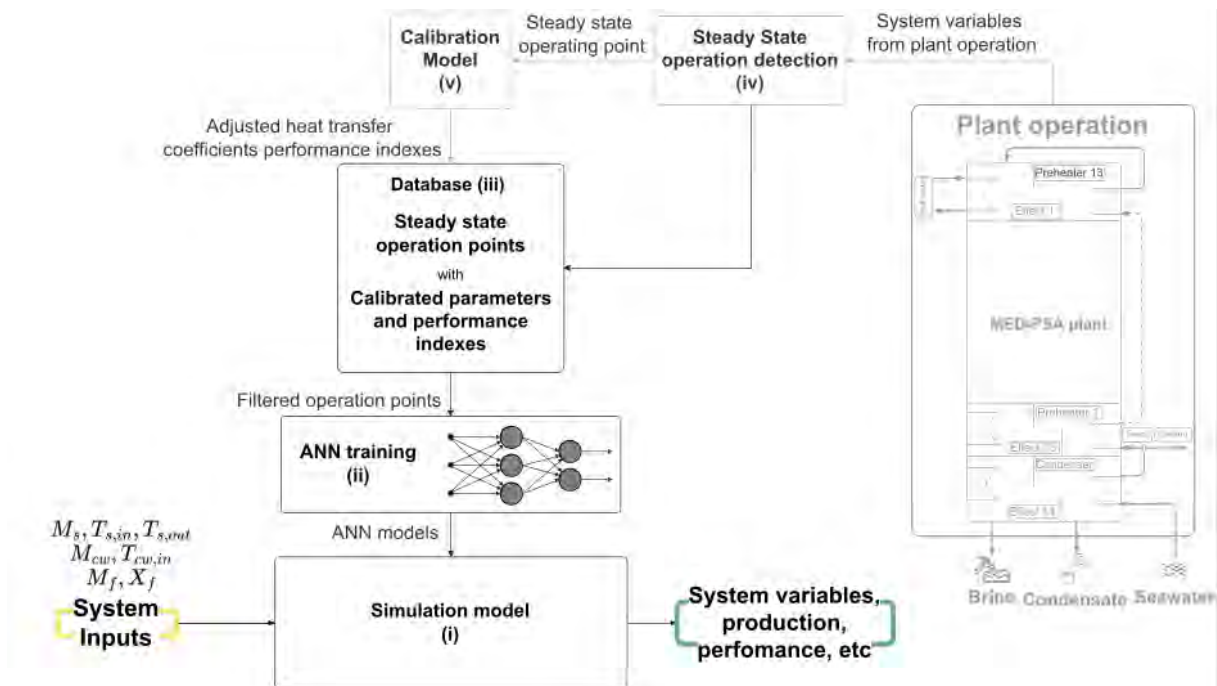


Fig 1: Methodology for the implementation of a steady state simulation model for an MED plant

- A methodology for the implementation of a data based steady state simulation model for an MED plant (see Figure 1). Different approaches are compared.
- The design and implementation of the MED unit low-level control in order to establish the operating point as well as the steady state operation and a web interface based on Python to monitor and interact with the system.

References:

- [1] E. Jones, M. Qadir, M. T. H. van Vliet, V. Smakhtin, and S. Kang, *Science of The Total Environment*, 657 (2019) 1343–1356
- [2] Q. Chen, M. Burhan, M. Shahzad et al., *Desalination*, 502 (2021)
- [3] Y. Zheng, R. Caceres Gonzalez, M. C. Hatzell, and K. B. Hatzell, *Applied Thermal Engineering*, 184 (2021)
- [4] *Concentrating Solar Power and Desalination Plants*, P. Palenzuela, D.-C. Alarcón-Padilla, and G. Zaragoza, Springer, 2015.
- [5] A. Christ, K. Regenauer-Lieb, and H. T. Chua, *Desalination*, 366 (2015) 47-58
- [6] D. Krishnamoorthy and S. Skogestad, *Computers & Chemical Engineering*, 161 (2022)

Implementation and evaluation of a solar photo-Fenton treatment plant for wastewater reclamation

Gualda-Alonso E.^{1,2}, Soriano-Molina P., Pichel N., Casas López J.L. and Sánchez Pérez J.A.

¹ Solar Energy Research Centre (CIESOL), Joint centre University of Almería – CIEMAT, Ctra. Sacramento s/n, Almería (Spain).

² Chemical Engineering Department, University of Almería, Ctra. Sacramento s/n, Almería (Spain). elizabeth.gualda@ual.es

The solar photo-Fenton process has been widely studied as a tertiary treatment for wastewater reclamation. Furthermore, the use of raceway pond reactors (RPR) to run the process has increased the attractiveness of the treatment with advantages such as the low construction cost, the high treatment capacities, or the ability to vary the liquid depth to achieve optimum use of photons [1]. Despite the large number of publications highlighting the efficiency of the process, the technical feasibility of using these reactors at large scale has not yet been demonstrated.

The main goal of this Ph.D. thesis is the implementation at demonstration scale of the solar photo-Fenton process as a tertiary treatment to reclaim wastewater for agriculture irrigation purposes. To this end, a RPR with a surface area of 100 m² was built in *El Bobar* wastewater treatment plant (WWTP), located in the city of Almería (Spain). The reactor is operated in continuous flow mode.

As a daily operation, the WWTP secondary effluent is led into a 5 m³ conditioning tank, where it is acidified at pH 2.8 with H₂SO₄. The pre-treated effluent is pumped into the reactor. The reagents are added by dosing pumps to the RPR inlet pipe. Finally, the water treated at acidic pH is neutralized at the outlet by passing through a calcium carbonate filter, increasing the pH up to 6.5. To work at the same rate of photon absorption, the liquid depth is set at 10 cm, in winter, and 18 cm, in summer. Based on the fluid dynamic of the 100-m² RPR and, considering that mixing time must be lower than the hydraulic residence time (HRT), the photo-reactor is operated at 60 min and 45 min of HRT, respectively, with 0.1 mM FeSO₄ and 1.47 mM H₂O₂. In order to verify the reclaimed water quality, samples were collected from the WWTP influent, WWTP secondary effluent, conditioning tank, RPR and water treated. The membrane filtration technique was employed for the enumeration of naturally occurring *Escherichia coli* (*E. coli*) and *Clostridium perfringens*, with a detection limit of 1 CFU/100 mL. Real contaminants of emerging concern (CECs) were monitored by direct injection in a LC-QqLIT-MS/MS system.

After running the solar photo-Fenton plant over one year, *E. coli* and *C. perfringens* disinfection attained > 5 and 2 log₁₀ reduction value (LRV), respectively, with regard to WWTP influent in

both winter and summer seasons. According to EU 2020/741 regulation [2], *E. coli* concentration in the photoreactor's effluent was within the monitoring requirements for reclaimed water quality Class A (≤ 10 CFU/100 mL), and therefore, also for the water classes with fewer quality restrictions (B, C and D). Concerning the CECs, up to 69 compounds, mainly pharmaceuticals and pesticides, were detected in the *El Bobar* WWTP secondary effluent, achieving removal percentages of 88% and 85% of the total load present in the secondary effluent in winter and summer, respectively.

Under these conditions, treatment capacities of $80 \text{ m}^3 \text{ day}^{-1}$, in winter, and $192 \text{ m}^3 \text{ day}^{-1}$, in summer, are estimated for 8 operating hours per day. The promising results in terms of secondary effluent disinfection and decontamination highlight the technical feasibility of the treatment for commercial application.



Fig.1. Solar photo-Fenton treatment plant at *El Bobar* WWTP, Almería city (Spain).

Acknowledgements. E. Gualda-Alonso appreciates the contribution of the LIFE ULISES project, funded by the European Union under Grant Agreement No. LIFE18 ENV/ES/000165. P. Soriano-Molina wishes to thank the Andalusian Regional Government for her research contract (DOC_00544) funded by the European Regional Development Fund through the Operational Programme 2014 – 2020, community measure D1113102E3. N. Pichel acknowledges the 'Juan de la Cierva' Program, Grant number FJC2019-042533.

References

[1] A. Cabrera-Reina, S. Miralles-Cuevas, J.A. Sánchez Pérez and R. Salazar, *Science of The Total Environment*, 800 (2021) 149653.

[2] EU 2020/741 of the European Parliament and of the Council of 15 May 2020 on minimum requirements for water reuse. *Official Journal of the European Union*. L 177/32, 5.6.2020.

New tertiary treatment for wastewater reclamation: Solar photo-Fenton combined with NaOCl

Solaima Belachqer-El Attar^{1,2}, Natalia Pichel^{1,2}, Paula Soriano-Molina^{1,2}, José Antonio Sánchez Pérez^{1,2}

¹Solar Energy Research Centre (CIESOL), Joint Centre University of Almería-CIEMAT, ²Chemical Engineering Department, University of Almería. E-mail address: sbe146@ual.es

The new European regulation (EU) 2020/741 [1] for reusing reclaimed water establishes more restricted requirements, concerning microbiological quality, to guarantee its safe use for agricultural irrigation. Water quality indicators for tertiary treatment plant validation include not only *Escherichia coli* (*E. coli*) but also more resistant microorganisms as coliphages and spore-forming sulfate-reducing bacteria, with disinfection targets $\geq 5 \log_{10}$ or absence. In addition, wastewater reclamation should consider the contaminants of emerging concern (CECs), which despite not being regulated yet, can cause serious human health problems and environmental damages [2]. In fact, they are being considered in the risk management of EU 2020/741. Hence, the development of low-cost and sustainable treatments is needed to comply with this new regulation. The solar photo-Fenton process is one of the most efficient advanced oxidation processes for removing CECs [2]. However, disinfection requires larger treatment times. Consequently, the need to investigate alternatives to reduce disinfection times arises. In this regard, a new solar photo-Fenton strategy based on the concurrent addition of hydrogen peroxide (H_2O_2), sodium hypochlorite (NaOCl) and ferric nitrilotriacetate (Fe^{3+} -NTA) has been recently proposed. This treatment allows to achieve the simultaneous disinfection and CEC removal in shorter times than solar photo-Fenton [2]. Therefore, this work aims to demonstrate the operational viability of this new solar photo-Fenton strategy in continuous mode for its applicability as tertiary treatment according to EU 2020/741.

Experiments were performed in 5-cm and 10-cm deep raceway reactors (RPRs) (19-L and 80-L total volume, respectively). The photoreactors were operated in continuous flow using actual wastewater treatment plant (WWTP) secondary effluents, which were spiked with the pesticide imidacloprid (IMD) (50 $\mu\text{g/L}$) and MS2 coliphage (10^7 - 10^{10} CFU/100 mL). Fe^{3+} -NTA (0.1 mM), H_2O_2 (1.47 mM) and NaOCl (0.134 mM), along with the WWTP effluent were continuously pumped into the reactor at 60-min hydraulic residence time [2]. Naturally occurring *E. coli* (10^1 - 10^3 CFU/100 mL), total coliforms (TC) (10^4 CFU/100 mL), *Enterococcus faecalis* (*E. faecalis*) (10^1 - 10^2 CFU/100 mL) and *Clostridium perfringens* (*C. perfringens*) (10^2 CFU/100 mL), MS2 coliphage, IMD, H_2O_2 , free chlorine, Fe^{3+} -NTA and total dissolved iron concentrations were determined at fixed time intervals throughout the treatment. The concentration of trihalomethanes (THMs) was also measured to monitor the formation/degradation of chlorination by-products.

The continuous flow operation of the photoreactor was evaluated over three consecutive days under an average solar UVA irradiance (327-380 nm) of 36 W/m². The operation started in batch for 60 min. Then, the feed pumps of reagents and wastewater were switched on, giving rise to the continuous flow operation, reaching the steady state in 30 min. Reagent steady state concentrations were 0.24 and 0.27 mM for H₂O₂, and 0.028 and 0.032 mM for total dissolved iron at 5 cm and 10 cm of liquid depth, respectively, and the residual free chlorine concentration was <0.01 mg/L. The steady state percentages of IMD removal were 82% and 75% in 5-cm and 10-cm deep RPRs, respectively. These values were kept for the second and third experimental days, pointing out the robustness of the treatment. Concerning disinfection, no differences were observed when reducing the liquid depth, with 2.6 log reduction value (LRV) for MS2, 1.2 LRV for *E. coli*, 1.5 LRV for TC, and 1.5 LRV for *E. faecalis*. *C. perfringens* showed resistance to the treatment process, undergoing no reduction. Validation of tertiary treatment technologies must be performed considering the concentrations of the raw water entering the WWTP [1]. In this regard, the total disinfection levels achieved were ≥5 log₁₀-units for *E. coli*, 2.8 LRV for TC, 4.7 for *E. faecalis*, and 3 for *C. perfringens*. Liquid depth was found to have a significant effect on the microcontaminant removal highlighting that operation at 10 cm of liquid depth is more feasible as the treatment capacity is higher than at 5 cm. In contrast, the disinfection could be mainly attributed to the disinfectant effect of chlorine.

Adjusting the oxidation conditions, this treatment is shown as a promising solution for water reclamation with the highest quality requirements (Class A). In addition, *E. coli* concentration in the photoreactor's effluent was within the monitoring requirements for Class A (≤10 CFU/100 mL), and THM concentration was 3 µg/L in the steady state below the limit established [3]. As concluding remark, these results encourage the future large-scale implementation of this treatment and further research in continuous-mode process optimization.

Acknowledgements: SferallIDC project (N° 823802). S. Belachqer-El Attar acknowledges the University of Almería (UAL18-BIO-A033-B), N. Pichel the 'Juan de la Cierva' Program (FJC2019-042533-I) and P. Soriano-Molina the Andalusian Government (DOC_00544).

References

- [1] Regulation (EU) 2020/741 for water reuse. J. Eur. Union. L 177/32, 5.6.2020.
- [2] S. Belachqer-El Attar, P. Soriano-Molina, I. De la Ojeda, J.A. Sánchez-Pérez. Sci. Total Environ. (2022), 155273.
- [3] Norme tecniche per il riutilizzo delle acque reflue, 99, 1, 3 aprile 2006, n. 152.

High temperature pressure sealing: Utilization in a receiver-reactor cavity system

Estefanía Vega Puga, Stefan Brendelberger

German Aerospace Center (DLR), Institute of Future Fuels, estefania.vegapuga@dlr.de

Solar thermochemical processes are considered promising technologies for cost-effective, large scale green hydrogen production, due to thermodynamic advantages compared to approaches based on photochemistry or electrochemistry [1]. For the implementation of thermochemical redox cycles in which the reactive material does not undergo phase change, different solar receiver-reactor concepts exist. Of those, three main approaches may be distinguished: *continuously rotating monoliths [2–4]*, *particle based with continuous feeding [5–8]* and *stationary monolith concepts with batch operation [9–12]*. Up to date, only limited efficiencies have been accomplished, with the batch operated cavity receiver-reactor concept *holding the highest demonstrated solar-to-fuel efficiency of 5.25 % [12]*.

With the aim of increasing the solar-to-fuel efficiency a new receiver-reactor concept was developed and presented in work of Brendelberger et al. [13]. The receiver-reactor reduces technical challenges associated with particle based or rotating concepts by keeping the transportation system elementary, while still benefiting from the high efficiency potential of incorporating two physically distinct reaction zones. The key features of the concept are movable reactive structures in combination with linear transportation systems and dedicated oxidation reactors. Unlike the state-of-the-art, the new concept allows for continuous on-sun operation leading to increased efficiency of the solar interface and permits options for solid heat recovery. Additionally, cyclic heating of the inert reactor vessel is avoided, achieving predicted efficiencies of above 14% even for non-optimized designs [13].

Our recent work focuses on the experimental demonstration of the aforementioned receiver-reactor cavity system, including a mobile redox unit with linear transportation system and oxidation reactor. Features of the system to be investigated incorporate atmosphere control and pressure sealing between reactors. Reliable and cyclic atmosphere separation between the two reaction zones has been identified as one of the main challenges, and therefore is being examined in detail. First experimental results on sealing materials that can sustain cyclic operation, high temperatures, steam and vacuum are presented. Four materials were tested in an experimental setup which comprises two separated zones that can be independently pressurised or vacuumed as well as a custom 3D printed valve that when open allows for fluid flow between zones. Correlations between pressure force and leakage rate are evaluated,

and ultimately, design choices for atmosphere separation within the receiver-reactor prototype are assessed.

References

- [1] A. Steinfeld, M. Epstein, *Chemistry in Britain* 37 (2001) 30–32.
- [2] R.B. Diver, J.E. Miller, M.D. Allendorf, N.P. Siegel, R.E. Hogan. *Journal of Solar Energy Engineering* 130 (2008), 041001.
- [3] R. B. Diver, J. E. Miller, N. P. Siegel, T. A. Moss, ASME 2010 4th International Conference on Energy Sustainability, Phoenix, USA, 2010.
- [4] H. Kaneko, Y. Ishikawa, C. Lee, G. Hart, W. Stein, Y. Tamaura, ASME 2011 5th International Conference on Energy Sustainability, Washington, DC, USA, 2011.
- [5] I. Ermanoski, N.P. Siegel, E.B. Stechel. *Journal of Solar Energy Engineering* 135 (2013), 031002.
- [6] S. Brendelberger, C. Sattler, *Solar Energy* 113 (2015) 158–170.
- [7] I. Ermanoski, J. Grobbel, A. Singh, J. Lapp, S. Brendelberger, M. Roeb, C. Sattler, J. Whaley, A. McDaniel, N.P. Siegel, Design and construction of a cascading pressure reactor prototype for solar-thermochemical hydrogen production, in: AIP Conference Proceedings 2016, 120001.
- [8] A. de La Calle, A. Bayon, *International Journal of Hydrogen Energy* 44 (2019) 1409–1424.
- [9] E. Koepf, S. Zoller, S. Luque, M. Thelen, S. Brendelberger, J. González-Aguilar, M. Romero, A. Steinfeld, AIP Conference Proceedings, Casablanca, Morocco, 2019, 2126.
- [10] S. Zoller, E. Koepf, P. Roos, A. Steinfeld. *Journal of Solar Energy Engineering* 141 (2019), 021014.
- [11] J.-P. Säck, S. Breuer, P. Cotelli, A. Houaijia, M. Lange, M. Wullenkord, C. Spenke, M. Roeb, C. Sattler, *Solar Energy* 135 (2016) 232–241.
- [12] D. Marxer, P. Furler, M. Takacs, A. Steinfeld, *Energy & Environmental Science* 10 (2017), 1142–1149.
- [13] S. Brendelberger, P. Holzemer-Zerhusen, E. Vega Puga, M. Roeb, C. Sattler, *Solar Energy* 235 (2022) 118–128.

Numerical investigation of a helically coiled solar cavity receiver for simultaneous generation of superheated steam and air

Yasuki Kadohiro, Timo Roeder, Kai Risthaus, Nathalie Monnerie, Christian Sattler

German Aerospace Center (DLR) - Institute of Future Fuels

Yasuki.Kadohiro@dlr.de

Concentrated solar thermal technologies have enormous potential to support achieving a carbon-neutral society. The high-grade thermal energy can be used directly for electricity generation or can provide process heat and thereby substitute fossil fuels. One promising application is the hydrogen generation in a solid oxide electrolyzer which requires high-temperature air and steam ($\sim 850^{\circ}\text{C}$). The solar receiver is an essential component in converting solar energy efficiently into thermal energy. Two basic receiver types exist: external and cavity receivers [1]. Among these two receivers, cavity receivers are considered highly efficient receivers since they can reduce heat losses and enhance the heat transfer efficiency to the thermal medium by insulating their surfaces except for an aperture [2]. Absorber tubes are most commonly used for cavity receivers due to a high efficiency and design flexibility [3].

So far, cavity receivers were utilized to heat a single medium [4,5,6]. However, it is likely to be beneficial to use a single receiver for steam generation and further heating of steam and air simultaneously. This allows different configurations that are assessed here.

In our study, a single cavity receiver that can conduct the following three processes: (i) water evaporation, (ii) superheating steam, and (iii) superheating air, is numerically investigated. The numerical model is verified with previously published data of a solar steam generator and superheater. The water evaporation and superheating steam processes were separated into different tubes since they are more economical, easy, and safe to operate [7]. The numerical investigation consists of three parts: (i) ray-tracing analysis, (ii) 3D steady-state thermal analysis, and (iii) 1D two-phase fluid flow analysis. These analyses were combined (i.e., solved sequentially or simultaneously) to investigate the receiver's performance (e.g., energy efficiency and loss, outlet fluid temperature). Three different cavity receiver structures, depicted in Fig.1, were developed and assessed. All of the receivers consist of a helically coiled tube due to their more compact design, easier manufacturing, and higher heat transfer performance compared to the straight tubes [8,9]. As shown in the figure, the receiver structure differs by the helically coiled tubes' shape and location. Receiver 1 consists of three horizontal helically coiled tubes. Each absorber tube corresponds to one heating process as indicated in the figure. Receiver 2 consists of three conical helically coiled tubes. The cavity's inner structure also has the conical shape. Receiver 3 consists of two horizontal and one conical helically coiled tube.

Our presentation shows the results of the numerical investigation and the assessment of the three designs regarding their performance, energy efficiency, thermal losses and achievable outlet temperatures. Thereby, our study helps designing cavity receivers for simultaneous heating of several media.

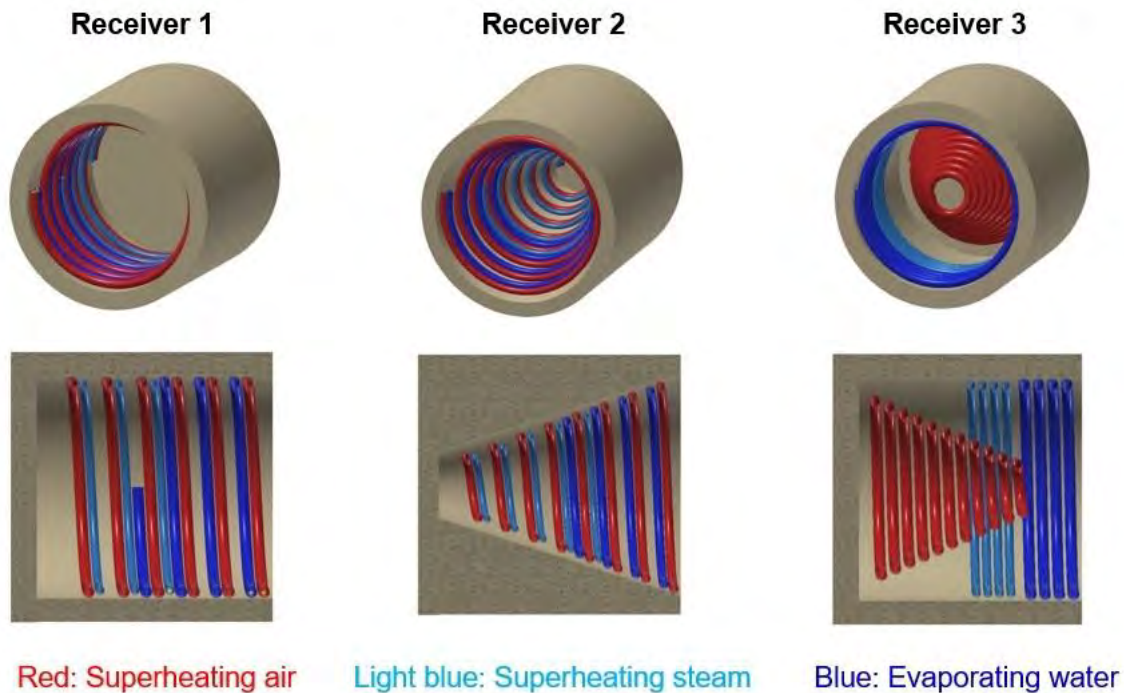


(Fig.1. Three different cavity receiver structures)

- [1] *Comprehensive energy systems*. I. Dincer, Netherlands, Elsevier Inc., 2018.
- [2] K. Kanatani, T. Yamamoto, Y. Tamaura, H. Kikura, *Solar Energy*, 153 (2017) 249-261.
- [3] K. Ho Clifford, D. Iverson Brian, *Renewable and Sustainable Energy Reviews*, 29 (2014) 835-846.
- [4] G. Schiller, M. Lang, P. Szabo, N. Monnerie, H. von Storch, J. Reinhold, P. Sundarraj, *Journal of Power Sources*, 416 (2019) 72-78.
- [5] M. Quero, R. Korzynietz, M. Ebert, A. A. Jiménez, A. Del Río, J. A. Brioso, *Energy Procedia*, 49 (2014) 1820-1830.
- [6] R. Uhlig, B. Gobereit, J. Rheinländer, *Energy Procedia*, 69 (2015) 563-572.
- [7] R. Ben-Zvi, M. Epstein, A. Segal, *Solar Energy*, 86 (2012) 578-592.
- [8] L. Santini, A. Cioncolini, M. T. Butel, M. E. Ricotti, *International Journal of Heat and Mass Transfer*, 92 (2016) 91-99.
- [9] J. Gou, H. Ma, Z. Yang, J. Shan, *Annals of Nuclear Energy*, 110 (2017) 648-667.

Optimization of Porous Structures for Enhanced Radiation Heat Transfer Using a Voxel-Based Ray-Tracing Algorithm

Sebastian Sas Brunser, and Aldo Steinfeld.

*Department of Mechanical and Process Engineering, ETH Zurich, Zurich 8092, Switzerland.
e-mail of presenting author: sasbrunser@ethz.ch*

Porous structures can enhance radiation heat transfer and thus the thermal efficiency of solar receivers for concentrated solar applications. To guide their design, we develop a pore-level ray tracer model that discretizes the domain into voxels, describing any complex geometry by simply defining which voxels are solid. Rays are then launched and traced through reflection, absorption, and reemission, solving the complete radiative heat transfer problem. The model can be further used with an optimization method to find the porous structure's optimum topology. An ideal optimization would prescribe the content of each voxel to maximize the mass above a threshold temperature while minimizing the temperature gradient across the resulting structure. However, because the radiative heat transfer model is nondifferentiable, analytical methods for optimization can't be applied.

We report on the model verification by comparing the results vs. those of a standard Monte Carlo ray tracer (VeGaS+). The porous structure used for this comparison consists of 351 identical overlapping opaque spheres, radius $R=31$ (voxels or meters depending on the model) on a $500 \times 500 \times 500$ voxels/meters domain. The resulting temperature distribution of both simulations closely matches. The model is coupled with a surrogate optimization method for a gradient-free maximization of an objective function.

Development of an experimental testbed for Pressurised Gas Solar Receivers using a High Flux Solar Simulator

David D'Souza^{1,2}, M.J. Montes^{1,2}, M. Romero¹ and J. González-Aguilar¹

¹High Temperature Processes Unit, IMDEA Energy, Avda. Ramón de la Sagra 3, 28935, Móstoles, Spain

²E.T.S. Ingenieros Industriales - UNED, C/Juan del Rosal 12, 28040 Madrid, Spain

Presenting author email: david.dsouza@imdea.org

1. Introduction

Gas phase heat transfer fluids are considered as one of the three development pathways of the next generation of Concentrated Solar Power (CSP) central receiver plants [1]. Using air as heat transfer fluids in solar receivers have several advantages as gases are generally chemical stable and non-corrosive across a wide range of temperatures and pressures besides being relatively inexpensive and environmentally non-hazardous. However, solar receiver design must consider the low thermophysical properties (thermal conductivity, density x specific heat) and handle properly pressure losses. In this regard, this work has focused on the analysis of microchannel receivers, which increase the heat transfer area by using compact structures [2]. Following the promising and novel results obtained using an in-house thermo-fluid numerical model of microchannel gas receivers, it proposes to design an experimental testbed capable of experimentally validating the findings of the simulations. This work has been developed within the framework of the ACES2030-CM project.

2. Experimental testbed

Employing the KIRAN-42 high flux solar simulator (HFSS) [3], with 7 lamps each of 6 kW (electrical) delivering a peak flux of over 3.5 MW/m² and approx. 14 kW radiative power on the focal plane, a calorimetric experimental facility has been developed and commissioned as shown in Fig.1. The experimental testbed has been currently assembled to use pressurised air from 5-25 bar at mass flow rates up to 2 g/s. The testbed was designed with the objective of flexibility in operating conditions. Thus a variety of absorber concepts may be tested individually or in combination (series/parallel) given the features of the multi-lamp high flux solar simulator and its intrinsically adaptable pointing strategies. The absorber's material (normally a metal alloy such as those from the Inconel or Haynes' series), surface coating, dimensions and internal flow geometry are some of the absorber properties that may be varied to understand their influence on its performance.



Fig.1. Experimental facility developed for gas phase receiver testing. (Left) KIRAN-42 High Flux Solar Simulator; and (right) Calorimetric testbed for receiver evaluation.

Relevant experiment data includes the pressure and temperature at the absorber inlet and outlet, the temperature and radiation flux profile across the irradiated surface and temperature gradient through the absorber bulk. Further processing may reveal performance indicators including thermal and exergy efficiencies, heat gain, pressure drop etc. Mechanical tests like ageing, external surface (coating) deformations may also be performed after multiple cycles.

Experiment plan

In previous studies, the thermofluid-dynamic performance of different compact structures, similar to those used in Plate Fin Heat Exchangers (PFHXs) have been compared, indicating the plain rectangular fin arrangement as one of the best in terms of thermal performance. In addition, the geometric parameters that most affect the receiver energy and exergy efficiency have been identified and optimised. The first samples to be tested are intended to prove these last results and validate the numerical model. Using a parametric analysis, varying the mass flow rate, incident radiation flux, operating pressure and temperature, a regression model may be developed to better understand the behaviour of the absorber.

References

- [1] M. Mehos, C. Turchi, J. Vidal, M. Wagner, Z. Ma, C. Ho, W. Kolb, C. Andraka, A. Kruienga. Report No. NREL/TP--5500-67464, 1338899 (2017).
- [2] S. Besarati, D. Yogi Goswami, and E. Stefanakos, *J. Sol. Energy Eng.*, 137, (2015) no. 3, p. 031018
- [3] J. Li, J. Gonzalez-Aguilar, and M. Romero, *Energy Procedia*, 69, (2015) 132–137

